



# THE UNIVERSITY *of* EDINBURGH

This thesis has been submitted in fulfilment of the requirements for a postgraduate degree (e. g. PhD, MPhil, DClinPsychol) at the University of Edinburgh. Please note the following terms and conditions of use:

- This work is protected by copyright and other intellectual property rights, which are retained by the thesis author, unless otherwise stated.
- A copy can be downloaded for personal non-commercial research or study, without prior permission or charge.
- This thesis cannot be reproduced or quoted extensively from without first obtaining permission in writing from the author.
- The content must not be changed in any way or sold commercially in any format or medium without the formal permission of the author.
- When referring to this work, full bibliographic details including the author, title, awarding institution and date of the thesis must be given.

*An Insight into the Regulation and Vulnerability of the Cyst Wall in Toxoplasma*

*Gondii*



THE UNIVERSITY  
*of* EDINBURGH

Toby Silva – S2275777

Masters of Research – Infectious Diseases

University of Edinburgh

Submitted in satisfaction of the requirements for the degree of MRes (Infectious Diseases) at

the University of Edinburgh

Year of Presentation - 2023

## Table of Contents

Abstract .....	4
Introduction .....	5
1.1 <i>Toxoplasma Gondii</i> Lifecycle – Acute to Chronic	
1.2 Protein Secretion and IVN	
1.3 GRA2	
1.4 Cyst Wall Proteins	
1.5 Phosphorylation	
1.6 GRA2 and CST1 regulation	
1.7 Aims and Results .....	18
Fig 1 – Analysis of Wildtype and Phosphomutant GRA2 constructs.	
Fig 2 – Comparing strategies for expressing HA-tagged GRA2 variants to complement $\Delta$ GRA2.	
Fig 3 - Confirmation of WT and phosphomutant GRA2 transfection and poor $\alpha$ -HA signal in tachyzoites and bradyzoites	
Fig 4 – Phosphomutant GRA2 in tachyzoites has little effect on localization in PV.	
Fig 5 – Targeting of <i>uprt</i> gene marker in creation of phosphomutants leads to abnormal ‘shrunk’ mature cysts.	
Fig 6 – Creation of $\Delta$ PPM3C.	
Fig 7 – Preliminary results $\Delta$ PPM3C leading to decrease of CST1 in cyst wall in mature cysts.	
Fig 8 – Plaque assay comparing gene deletion and wildtype parasites after acid digestion.	
Discussion .....	44
Materials and Method .....	57
References .....	67
Supplemental Figure .....	79

Declaration

The following thesis and all work detailed has been completed by me except  
Immunofluorescence Microscopy images captured by Post Doc. Kseniia Bodnarenko.

Such work is to be submitted only for an MRes Infectious Diseases degree.

Toby Silva – 30.08.2023

## Abstract

*Toxoplasma gondii* is a parasite belonging to the apicomplexan family and is capable of intracellular invasion. The parasite can secrete a multitude of different proteins that aid its cause in infecting nucleated host cells. This is seen not only during the acute phase (tachyzoite) but also the latent (bradyzoite) phase. Here, the parasite is known to form cyst structures, where they encapsulate and safely evade the immune host response. Cysts can persist for the entirety of the host lifecycle. Critically, there is no current treatment and reactivation of these cysts is heavily linked to human disease. Secreted proteins are vital to parasite function in both chronic and acute infection. GRA2, is a dense granular protein secreted by the parasite. GRA2 can induce the formation of the intravacuolar tubular network (IVN), an important structure in intracellular tachyzoites. Crucially it can localize to the cyst wall alongside another secreted protein, CST1, in bradyzoites. This highlights a dynamic behaviour in both stages of the life cycle, previous phosphoproteomics show that proteins are differentially phosphorylated in acute and chronic infection. We hypothesize such phosphorylation has a large impact on protein localisation in the parasite during infection stages. Additionally, we argue the importance of key modulatory enzymes such as phosphatases to also play a role in this process. In our experiments, we successfully created and transfected phosphomutant GRA2, via target of the uprt gene marker. Using immunofluorescence microscopy, we show that  $\alpha$ -HA is a poor probing method in comparison to  $\alpha$ -GRA2. Importantly we show disruption of the uprt gene marker, whilst validated during our initial transfection experiments, is detrimental to bradyzoite differentiation in mature cysts. Finally, after investigating a previously described phosphatase, PPM3C, we produced preliminary findings showing that  $\Delta$ PPM3C impacts the localisation of CST1 at the cyst wall in mature cysts.

Word Count – 16,000

**Keywords:** *Toxoplasma gondii*, **GRA2**, **dense granule**, **phosphorylation**, **regulation**, **secreted proteins**, **cyst wall**, **phosphatase**, **PPM3C**, **plaque assay**.

# An Insight into the Regulation and Vulnerability of the Cyst Wall in *Toxoplasma Gondii*

## 1. Introduction

*Toxoplasma gondii* is an obligate intracellular parasite of the Apicomplexan family (Zhang et al., 2019). It infects one-third of the human population, and although appears asymptotically in immunocompetent hosts, it is able to cause severe disease in the immunocompromised (Hokelek, 2019). The parasite is commonly seen with three clonal lineages (types I, II and III) with prevalence of these three observed highly in Europe and America (Sibley and Ajioka, 2008). Cancer and HIV patients are classified as vulnerable, with infection of the central nervous system the most common here. (Ayoade and Joel Chandranesan, 2023). In addition, ~40% of AIDS patients are known to present with encephalitis (Kotra, 2007). During pregnancy, infection can result in transmission across the placenta to the fetus, leading to congenital toxoplasmosis. During infection this typically manifests with neural defects (Stray-Pedersen, 1993). The parasite is readily able to infect livestock - highlighting an economical issue as well as a health burden (Stelzer et al., 2019).

### 1.1 *Toxoplasma gondii* Lifecycle – Acute to Chronic

*Toxoplasma* has a complex biphasic lifecycle with sexual reproduction occurring in felids and asexual replication in a range of intermediate hosts (Frenkel, 1973). Passing of feces from the felid results in excretion of a large number of oocysts. Oocysts, once sporulated give rise to infective sporozoites, which upon inhalation or ingestion into an intermediary host – gives the parasite a means of asexual reproduction (Aguirre et al., 2019). It is the result of such asexual reproduction that leads to prevalent human and animal disease. Infection into humans is commonly seen via the ingestion of undercooked meats, or drinking

sources of contaminated water and unpasteurized milk products (Stelzer et al., 2019). Ingestion of oocysts will result in their degradation by enzymes located in the digestive tract (Attias et al., 2020). This causes the release of sporozoites or bradyzoites that are able to invade host cells and convert to tachyzoites, this is responsible for the acute phase of infection. Intracellular invasion is accomplished via microneme proteins (AMA1 and MIC2) inserted into the membrane of the tachyzoite, and are able to recognize and attach to host cell receptors (KATO, 2018). Other secretions from the parasite aid a complex called the Moving Junction (MJ) to internalize the parasite. During this complex invasion process, the parasitophorous vacuole (PV) forms (Sinai, Webster and Joiner (1997). The surrounding Parasitophorous Vacuole Membrane (PVM) forms and behaves as a barrier between the host cell cytoplasm and the PV, which now becomes the replicative niche of the parasite (Clough and Frickel, 2017). Egress of *Toxoplasma Gondii* occurs once the host cell can no longer support the growth and proliferation of parasites. This causes rupturing of host cell machinery and structure, and critically leads to the repeating cycle of invasion (Dubey, Lindsay and Speer, 1998).

As parasite replication increases, a host immune response is observed resulting in the clearing of tachyzoites. However, a small population of parasites are able to resist and survive such mechanisms. It is here, where research argues tachyzoites undergo differentiation into the slower growing and replicating bradyzoites (Jeffers et al., 2018). Parasites are now able to encapsulate in cysts and are protected by a thick cyst wall, described as a rigid and a modified version of the PVM (Sullivan and Jeffers, 2012). Previous work demonstrates that within the cyst wall, bradyzoites are connected together and to the cyst wall by specialized tubules that form an intracyst network (ICN) or cyst matrix (Lemgruber et al., 2011). Ultimately, this form of

*Toxoplasma* is able to successfully evade the immune responses elicited by the host, ensuring persistence of parasite infection. Stage conversion is associated with differential gene expression resulting in morphological and structural changes (AdomAko-Ankomah, Wier and Boyle, 2012). (Radke et al., 2005) highlighted the major role of differential gene expression in *Toxoplasma*, specifically regarding increase/reduction of gene transcripts during stage conversion. One key feature of bradyzoites is an altered metabolism, aligning with their slower replicative rate (Hargrave et al., 2019). Expectedly, research found transcription products from genes relating to metabolism as well as cell and DNA replication were downregulated compared to tachyzoites. Such findings strongly support the slow replicating characteristic of latent infection as well as differential gene expression. However, differentiation of bradyzoites is still to be fully understood, one suggested model discusses activation of stress response genes (SRG's). Activation of SRG's in response to host immunity, alongside the integration of stimuli are argued to produce phenotypic changes that are associated with bradyzoites (Singh, Brewer and Boothroyd, 2002). Critically to the parasite lifecycle, this differentiation is reversible, with the reactivation of cysts leading to outbursts of infection by the infective tachyzoites (Cerutti, Blanchard and Besteiro, 2020). Whilst rupturing of cysts does occur naturally and spontaneously, the clearance of tachyzoites by a working and effective immune system will result in minimal complications for the host (Soete et al., 1993). Infected hosts who are immunocompromised/suppressed will find themselves unable to rid the reactivated tachyzoites. Those who lack a capable immune system are susceptible from serious manifestations of toxoplasmosis - commonly presenting with encephalitis, pneumonia and retinochoroiditis (Machala et al., 2015).

## 1.2 Protein secretion and IVN

*Toxoplasma gondii*, is known to secrete a plethora of proteins to aid in survival and proliferation. The tachyzoite contains a cone shaped tip termed the conoid and is argued to be one of the first points of contact to host cell cytosol during invasion. This conoid contains a number of multiple secretory organelles called Rhoptries. As well as aiding with invasion, the rhoptries secrete proteins with the function of manipulating host cells to sustain infection (Montoya, Boothroyd and Kovacs, 2015). Shortly after the formation of the PV, the tachyzoite is known to develop a network of intravacuolar tubules (IVN). (Magno et al., 2005) proposed a model for the IVN, where it is hypothesized to confer structural rigidity to the tachyzoite. This is supported by (Tosetti et al., 2019), showing presence of filamentous actin (F-actin) within the IVN tubules. The presence of such F-actin is shown to regulate the stability and structure of the tubules. The IVN is also seen to contribute to the development of intracellular parasites, via the uptake of nutrients from the host cell cytoplasm (Bai et al., 2018). Parasites that were unable to form proper IVN structure, due to gene deletion, showed a reduction in host cell protein uptake (Romano et al., 2017). Dense granular proteins (GRA's) are a majority of secreted proteins by the parasites. Some of which have a shared function to aid maturation of the PV. An example is GRA7 that is observed to deform liposomes near the IVN as well as being able to recruit host lysosomes to the PV (Coppens et al., 2006). Another is GRA6, seen to additionally aid the reshaping of vesicles into stable nanotubules, aiding IVN development (Lopez et al., 2015). (Mercier et al., 2002) showed parasites lacking GRA6 contained IVN structures exhibiting abnormal phenotype. Instead, the IVN was seen to be disconnected and vesicles and were no longer part of an extensive network of tubules, as seen in normal tachyzoites. GRA2

is one such protein that is closely associated with the IVN following its secretion. Certain GRA's are labelled as IVN GRA's due to the strong association to the IVN in acute infection. GRA's are also observed to colocalize and form complexes with one another; GRA2, GRA4 and GRA6 is an example of an observed multimeric complex. This complex is hypothesized to have a strong association with the IVN, supporting the shared function of IVN GRA's (Nam, 2009). Taken together, the IVN and the proteins secreted from the parasite here are critical to *Toxoplasma Gondii* in the acute stage (Dou et al., 2014).

### 1.3 GRA2

GRA2 is a 25kDa hydrophobic protein (Golkar et al., 2007), it is 185 amino acids in length and structurally is predicted to contain 3 amphipathic helices ( $\alpha^1$  residues 69-87), ( $\alpha^2$  residues 98-116), ( $\alpha^3$  residues 119-139). It was found that either side of these helices, are predicted to be hydrophilic regions (Travier et al., 2008). Previous work has also outlined that these helical regions are essential for GRA2 function (Mercier, Cesbron-Delauw and Sibley, 1998). The evidence provided highlighted that deletion of any of the three helical regions led to a lack of IVN formation in the PV and as a result, reduced protein uptake. These findings were supported by (Bittame et al., 2015) showing that removal of these amphipathic helices (AH's) led to a GRA2 protein that were structurally abnormal. Such mutant GRA2 resulted in a disorganized IVN in tachyzoites and again affected protein uptake. Protein re uptake from host cytoplasm is vital in order to aid maturation of the PV (Travier et al., 2008), elucidating that GRA2 is a critical secreted protein in tachyzoites. Deletion of the *gra2* gene entirely was also shown to result IVN membranes becoming abnormally large vesicles rather than highly curved, affecting PV organization (Sibley et al., 1995). All are key studies supporting the importance of

GRA2, in relation to IVN formation. In contrast to other IVN associated GRA's, GRA2 is also seen in abundance during the chronic stage. It is seen at the cyst matrix and wall, at day 2 and 7 post differentiation *in vitro* respectively (Guevara et al., 2019). Here researchers were able to show  $\Delta$ GRA2 parasites formed abnormal cyst matrix structures. One key finding in particular showed that movement of GRA2 to the cyst wall, also enabled colocalization of other secreted proteins here. This raises the possibility that arrest of GRA2 movement to the cyst wall may impact movement of other key cyst wall proteins. The movement of GRA2 at both acute and chronic parasite infection indicates the protein must be dynamically regulated. Importantly, there is a current gap in understanding the molecular mechanisms behind such movement, this is something we aim to bridge in our work. During the chronic stage, *Toxoplasma* secretes a number of proteins that are localized to the matrix of the cyst as well as the periphery of the cyst wall. CST2 and CST3 are such proteins described by (Tu et al., 2019). Deletion of such proteins did not show evidence of weakened or abnormal phenotype cyst structure, however there was a noticeable reduction in virulence *in vivo*. This evidence stipulates that previously characterized chronic stage secreted proteins may share important functions at the acute stage. Such a finding raises the distinct possibility that other secreted proteins behave dynamically, in a similar manner to GRA2.

#### 1.4 Cyst Wall Proteins

Perhaps the most critical protein within the cyst wall is CST1, it is characterized as a 2451 amino acid protein. Classed as a highly glycosylated protein, CST1 is argued to be a major structural component of the chronic cyst wall (Weiss, 2000). CST1 contains a mucin-domain, and research has shown this is vital in relation to forming a rigid cyst wall (Tomita et al., 2013). Mucin domains are known

to have serine and threonine rich regions, and they represent a family of glycoproteins that are known to possess a considerable number of GalNAc O-glycosylation's (Tomita et al., 2017). Thanks to the level of glycosylation here, researchers postulate that CST1 is significant in conferring cyst wall durability. Evidence from the described research attributes rigidity of the cyst wall to CST1 and its ability to bind *Dolichos Biflorus lectin* (DBA) as well as succinylated germ agglutinin. These bindings are hypothesized to additionally confer evasion from host immune response, as well as structural rigidity (Tu, Yakubu and Weiss, 2018). Production of CST1 at the chronic stage is vital, (Tomita et al., 2013) show that chronic cysts lacking CST1 are reduced, not only in number, but exhibit a weakened structure. This is observed to have a thin and misshapen phenotype in contrast to normal cyst walls with prominent and thicker appearance.  $\Delta$ CST1 parasites were also seen to have a cyst wall that contained a disrupted layer of other glycosylated proteins (Tomita et al., 2013), supporting the theory of protein colocalization here. The upregulation of the gene responsible for CST1 in bradyzoites (Young et al., 2020) and lack of observed expression seen in tachyzoites indicates that stringent regulation is involved here. These are strong indications that both CST1, and the above mentioned GRA2, behave dynamically throughout the lifecycle of *Toxoplasma Gondii*. Furthermore, this validates our investigation into parasite regulation, data here could be critical in understanding the behavior of other related secreted proteins. As of now, chronic stage toxoplasmosis remains an untreatable condition, defining regulation and movement of secreted proteins could aid the development of therapeutic targets in chronic infection.

## 1.5 Phosphorylation

It is widely accepted that phosphorylation occurs to a large number of the secreted proteins from *Toxoplasma Gondii* (Treeck et al., 2011). It is the most common method of regulating protein function within eukaryotes and is usually responsible for the movement/targeting of proteins to specific locations within cells, post secretion. These modifications are thought to play an essential role in response mechanisms deployed by the parasite to stimuli in the host cell environment (Bougdour et al., 2010). In addition to localization and movement of proteins, these regulatory mechanisms are thought to affect stability of proteins as well as their interactions with other proteins (Yin et al., 2022). It is important to note that phosphorylation is not the only key post translational modification (PTM) that occurs within the parasite lifecycle. Other well-known PTM's that have been discovered are malonylation (Nie et al., 2020), ubiquitination, methylation (Yin et al., 2022) and O-GlcNAcylation (Wang et al., 2016). Further phosphoproteomic analysis of the *Toxoplasma* and *Plasmodium Falciparum* genome (Treeck et al., 2011) shows evidence that phosphorylation is a highly conserved PTM in the apicomplexan family. Phosphorylation would not be possible without the use of Protein Kinases (PK) and Phosphatases (PP), that are critical in the PTM process. Classes of protein kinases are able to transfer a phosphoryl group to a hydroxyl group of a protein substrate, via an ATP molecule (Gaji, Sharp and Brown, 2021). These events occur at three specific chains of amino acids: serine, threonine, and tyrosine (Ardito et al., 2017). Once transfer of a hydroxyl group is completed by an effector, the PTM process is finalized resulting in the substrate proteins activity, movement, or interaction with other intracellular components (Manning, 2002). Phosphatases are an effector that is argued to play a key role in the lifecycle of *Toxoplasma*.

Serine/Threonine Phosphatases (PSP's) are seen most commonly in infection processes, this is argued due to the high prevalence of serine and threonine residues in secreted proteins (Jacot et al., 2014). Calcineurin is one such discovered PSP and is a calcium regulated phosphatase (Dobson et al., 1999), it is found to regulate functions of parasite-host cell attachment. (Paul et al., 2015) discovered that such a PSP was also found in *Plasmodium Falciparum* aiding host cell interactions, highlighting conserved function within the apicomplexan family. *Toxoplasma Gondii* secretes ~ 50 protein kinases and phosphatases (Peixoto et al., 2010). An example of PSP regulation relates to the aforementioned microneme proteins involved with invasion, the AMA-RON complex and PPM5C (Yang et al., 2019). Research is able to show the critical nature of PPM5C, a PSP, where parasites lacking the catalytic domain were subsequently unable to attach to host cells effectively. Taken together, findings as outlined above validate the need to further research the function of other phosphorylation effector enzymes. Similar to PPM5C, PPM3C, is secreted by *Toxoplasma* and contains a domain sharing homology with the PP2C family of serine/threonine phosphatases (Mayoral et al., 2020). This superfamily of phosphatases is known to share eleven conserved motifs between them (Bork et al., 1996). Although confirmed not to be involved with host cell attachment, like PPM5C,  $\Delta$ PPM3C parasite cultures led to discovery of an abundance of phosphopeptides (Mayoral et al., 2020). Phosphopeptides are a key indicator of PTM, and such a discovery was related to the secretions of vacuolar proteins. Significantly in relation to our research, phosphopeptides from GRA2 were discovered as well as phosphopeptides from PPM3A, another PSP. This specific finding hints that communication between phosphatases may occur during secretion. The data also revealed phosphopeptides of other secreted vacuolar proteins, suggesting there may

be numerous potential protein substrates of PPM3C. The investigation additionally highlighted the presence of mRNA transcripts from PPM3C in both tachyzoite and bradyzoite stages of infection. Supporting an argument put forward, that PPM3C is clearly active throughout the parasite lifecycle (Mayoral et al., 2020). Unfortunately, researchers were unable to fully confirm that GRA2 is a protein substrate of PPM3C. It must be noted that these conclusions were drawn from the data of  $\Delta$ PPM3C parasite cultures at a specific time point, 32 hours post infection. This leads to a distinct possibility that dysregulation of the GRA2 protein could occur at a different time point later in tachyzoites or even during the chronic infection. This in particular is a gap in information that we aim to build upon in our research. We believe that PPM3C may be an important phosphatase used in the regulation of secreted proteins, namely GRA2. By closely examining the relationship, such findings would help determine whether GRA2 is a substrate of PPM3C during the parasite life cycle. Additionally, we sought to gather evidence that phosphatases are secreted together and 'crosstalk' with one another during the infection cycle of *Toxoplasma Gondii* (Mayoral et al., 2020).

### 1.6 GRA2 and CST1 regulation

GRA2 is found to have numerous potential residues that could be susceptible to modification by protein kinases and phosphatases. These specific residues within a secreted protein are termed here as 'phosphosites' and they may exert a degree of control over function and movement of the protein. Residues that are susceptible to phosphorylation/dephosphorylation could result, for example, in the GRA2, GRA6 complex association with the IVN (Fox et al., 2019). Another example could be hypothesized in the chronic stage, leading to the colocalization of GRA2 and other cyst wall proteins to the cyst wall or matrix. This working hypothesis arises from

previous work into phosphosites of significance that were discovered in the *Toxoplasma* genome (Young et al., 2020). Interestingly, data was able to show that several GRA proteins are differentially phosphorylated between the acute and chronic infection. GRA2 is shown to have three phosphosites of significance – two of these are located within the region of GRA2's first amphipathic helix. It is well known that membrane recognition/insertion and binding are the primary functions of such helices (Drin and Antonny, 2009). Phosphosites predicted within this region could be used to regulate function of AH's during IVN association. This theory supports the established behavior of GRA2, whilst outlining another hypothesis - that phosphorylation could be the driving biological process behind IVN association of GRA2. Like GRA2, the (Young et al., 2020) phosphoproteomic data indicates residues within the CST1 protein that are targeted for phosphorylation. Unlike GRA2, after analyzing the secondary structure of CST1 ([heliQuest](#) - Gautier et al., 2008) there are no indications of amphipathic helices. However, the protein contains 13 SRS(Surface antigen-1 related sequence) domains, which are argued to aid in attachment to host cells, as well as immune response evasion (Tomita, Ma and Weiss, 2018). The previously described mucin domain as previously mentioned, is critical to the persistence of the parasite during latent infection. Mucin domains such as the one described in CST1 are also associated with the protection against proteases in the gut, which would be secreted during transmission here (Mortara et al., 1992). Movement of dynamic proteins within the parasite must stringently controlled, supporting the need to examine the role phosphorylation in detail. We hypothesize that this PTM is one of the key mechanisms involved in restructuring and regulation of secreted proteins in *Toxoplasma Gondii* during its complex lifecycle. Uncovering, in depth, these mechanisms behind regulation could be of

critical use in the development of specific and preventative treatment towards toxoplasmosis.

### 1.7 Aims and Results Overview

To investigate phosphoregulation within the forming cyst we directly investigated phosphorylation of secreted proteins and the impact of phosphatases in *Toxoplasma gondii*. Our primary aim was to determine if previously described phosphosites found within GRA2 engaged in the protein's dynamic movement. This resulted in the creation of phosphomutant GRA2, via SDM. In addition, we wanted to view the role of phosphatases such as PPM3A and PPM3C, viewing how gene deletions of these phosphatases impact one another as well as GRA2. We wanted to view how these phosphomutant proteins and gene knockouts could also affect bradyzoites and the cyst wall. A secondary aim was to assess how we could assay genetic deletions in parasite lines. This involved investigating the durability of the cyst wall structure after exposure to external stress. To do this we would evaluate a method of biochemical digestion, and use microscopy after fixing/staining to observe plaquing ability.

Our results initially helped to validate a strategy of inserting wildtype and phosphomutant GRA2-HA into Me49 $\Delta$ ku80 $\Delta$ GRA2 parasites. Specifically, via pCas9 targeting of uprt, instead of the initially tested hxgprt gene marker. We additionally discovered that  $\alpha$ -HA probing was a poor choice to visualize our GRA2 constructs. However, our final discovery regarding phosphomutant GRA2 emphasizes that target of the uprt gene marker is detrimental, in regard to bradyzoite differentiation. Earlier tachyzoite and bradyzoites exhibit no phenotype when transfected with phosphomutant GRA2. The phenotype caused by the uprt gene marker disruption unfortunately prevented further analysis of phosphomutant GRA2 in mature cysts.

Creation of  $\Delta$ PPM3C parasites allowed analysis of the phosphatase and its potential relationship with GRA2. We were unable to create  $\Delta$ PPM3A, therefore a potential relationship between the two phosphatases could not be determined. Although no such relationship was concluded between PPM3C and GRA2 during tachyzoite or bradyzoite differentiation. We were able to show preliminary findings that  $\Delta$ PPM3C affects the structure of the cyst wall in day 7 bradyzoites, specifically with loss of CST1.

Our plaque assay results were unconvincing in an attempt to assay cyst wall and genetic deletions. However, we validate further improvement of protocol to highlight the potential importance of secreted proteins in *Toxoplasma Gondii*.

## Results

In order to investigate the potential role of phosphorylation in the localization of GRA2 in the forming cyst we identified 3 phosphosites that were found to be differentially phosphorylated in the *Toxoplasma* lifecycle. Previous phosphoproteomic data (Young et al., 2020) listed 3 sites of interest for our work - Threonine 56 (T56), Serine 72 (S72) and Serine 76 (S76). We sought to modify the wild type residues (Serine/Threonine) that were found in the gene encoding ([TGME49\\_227620](#)) for GRA2. Phosphoproteomics highlighted an exponential increase of phosphorylation of T56 in bradyzoites, whilst S72 and S76 show an increase of phosphorylation in tachyzoites. Creation of a phosphomimetic GRA2 at these sites required substitution of Aspartic Acid, whilst phosphoablative GRA2 needed Alanine.

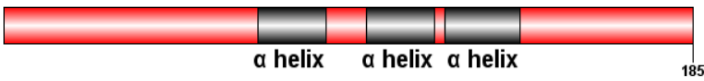
Site directed mutagenesis (SDM) would allow for targeting of specific residues within the amino acid chain. To induce these changes, SDM required custom designed oligonucleotide primers (listed in Table S1 and created with [NEBaseChanger](#)). Primers were ordered in a back-to-back manner as opposed to an overlapping orientation to increase transformation efficiency according to Q5 SDM kit protocol (NEB, Biolabs). This resulted in 2 versions of phosphomutant GRA2 with S72 and S76 substituted for Alanine (phosphoablative GRA2) and GRA2 with S72 and S76 substituted for Aspartic (phosphomimetic GRA2) (Fig 1A). Primers that were designed to create phosphomutant T56 were not confirmed via sequencing, after multiple SDM and transforming attempts. Therefore, experiments continued forward with phosphomutant S72 and S76 sequences only. To aid localization all transfected sequences were tagged with a single copy of the hemagglutinin epitope (HA). To ensure that only phosphomutant versions of the protein were expressed at any point, we aimed to complement GRA2 into Me49 $\Delta$ ku80 $\Delta$ GRA2 parasites.

The presence of three amphipathic helices within the structure of GRA2 is vital for association to the IVN (Mercier, Cesbron-Delauw and Sibley, 1998). (Fig 1B) details the amino acid translation of wild type GRA2 from amino acid residues 68-143. Domains of amphipathic helices are represented below amino acid translation as stated by (Travier et al., 2008). Our successful SDM experiments of S72 and S76 are located within the region of the first amphipathic helix. Helical wheels are drawn above to represent the result of such mutagenesis – mutating wildtype serine residues to alanine/aspartic. Predicted analysis of mutagenesis is carried out via the online heliQuest tool ([heliQuest](#) - Gautier et al., 2008). Use of the server allows the user to input an amino acid sequence, resulting in calculation of physiochemical properties of the protein. Importantly of use to our work, this server contains a ‘mutation module’ whereby the user may mutate helices manually to compare with the original sequence. Another feature of the server is calculation of a predicted hydrophobic moment ( $\mu\text{H}$ ).  $\mu\text{H}$  is often used to measure the hydrophobicity or hydrophilicity of a region within an amino acid chain (Eisenberg, Weiss and Terwilliger, 1982). A useful tool for researchers regarding prediction of proteins, their potential interactions as well as their respective functions. The helical wheels also allow an illustration of the spatial relationships between amino acids in a region, with our interest being in the first amphipathic helix of GRA2. The arrow of the helix points the direction of the helix (from N- terminus towards the C-terminus) indicating where the moment of peak hydrophobicity falls. The arrangement of the amino acid residues allows insight into how they interact with one another (Gutte and Klauser, 1995). Average hydropathy (H) is another feature of the prediction tool, assigning a numerical value to amino acids based on their hydrophobicity/hydrophilicity. In (Fig 1B)  $\mu\text{H}$  and H are assigned to the amino acid of which the arrow points towards,

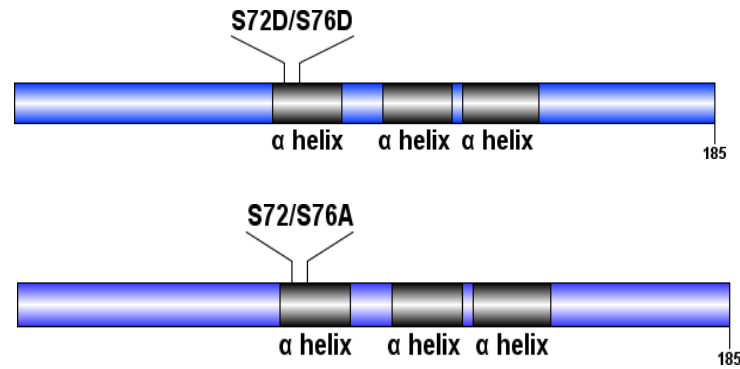
indicating the peak hydrophobic moment of the helix. The helical wheel representing phosphoablative S72 and S76, shows no difference regarding the direction of the predicted helix structure. However, an increase in hydrophobic moment and decrease in average hydrophobicity are seen. A trend was seen in (Eisenberg, Weiss and Terwilliger, 1982) where an  $\mu H$  value  $>0.5$  and H value of 0.2 would indicate membrane interaction from a protein. Certainly, it would prove to be interesting if this finding was to be translated, observing the behavior of phosphoablative GRA2. Prediction of the aspartic mutation results in a helical wheel showing a similar increase/decrease of  $\mu H$  and H values. One difference is a slight shift of helix direction, pointing towards the Phenylalanine (F) amino acid in comparison to the wildtype and phosphoablative GRA2 predictions. To move forward with visualizing if these changes translate to a phenotypic change in localization of GRA2 *in vitro*, we must first consider our strategy of inserting GRA2 variants into parasites.

A

WT – GRA2

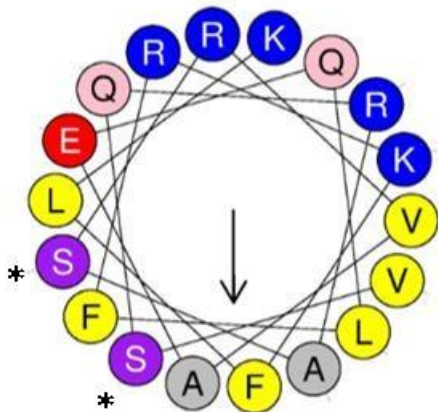


Phosphomutant – GRA2



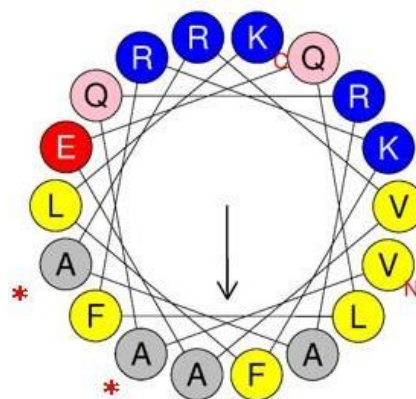
B

WT GRA2


 $\mu\text{H} - 0.215$   
 $\text{H} - 0.519$ 

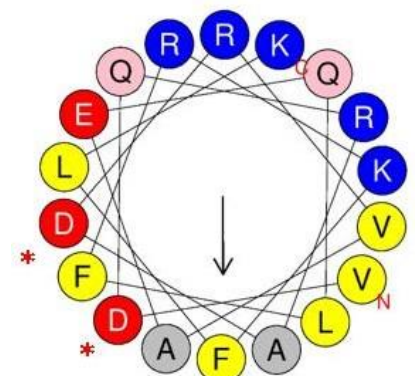
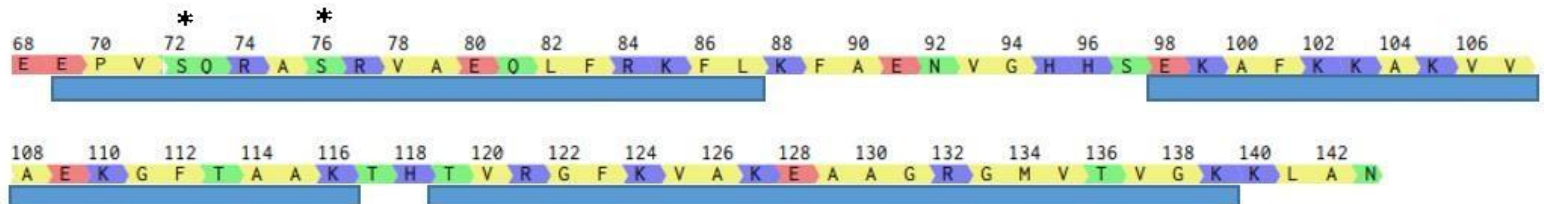
Phosphoablative GRA2

(Alanine Mutation)


 $\mu\text{H} - 0.542$   
 $\text{H} - 0.254$ 

Phosphomimic GRA2

(Aspartic Mutation)


 $\mu\text{H} - 0.478$   
 $\text{H} - 0.134$ 


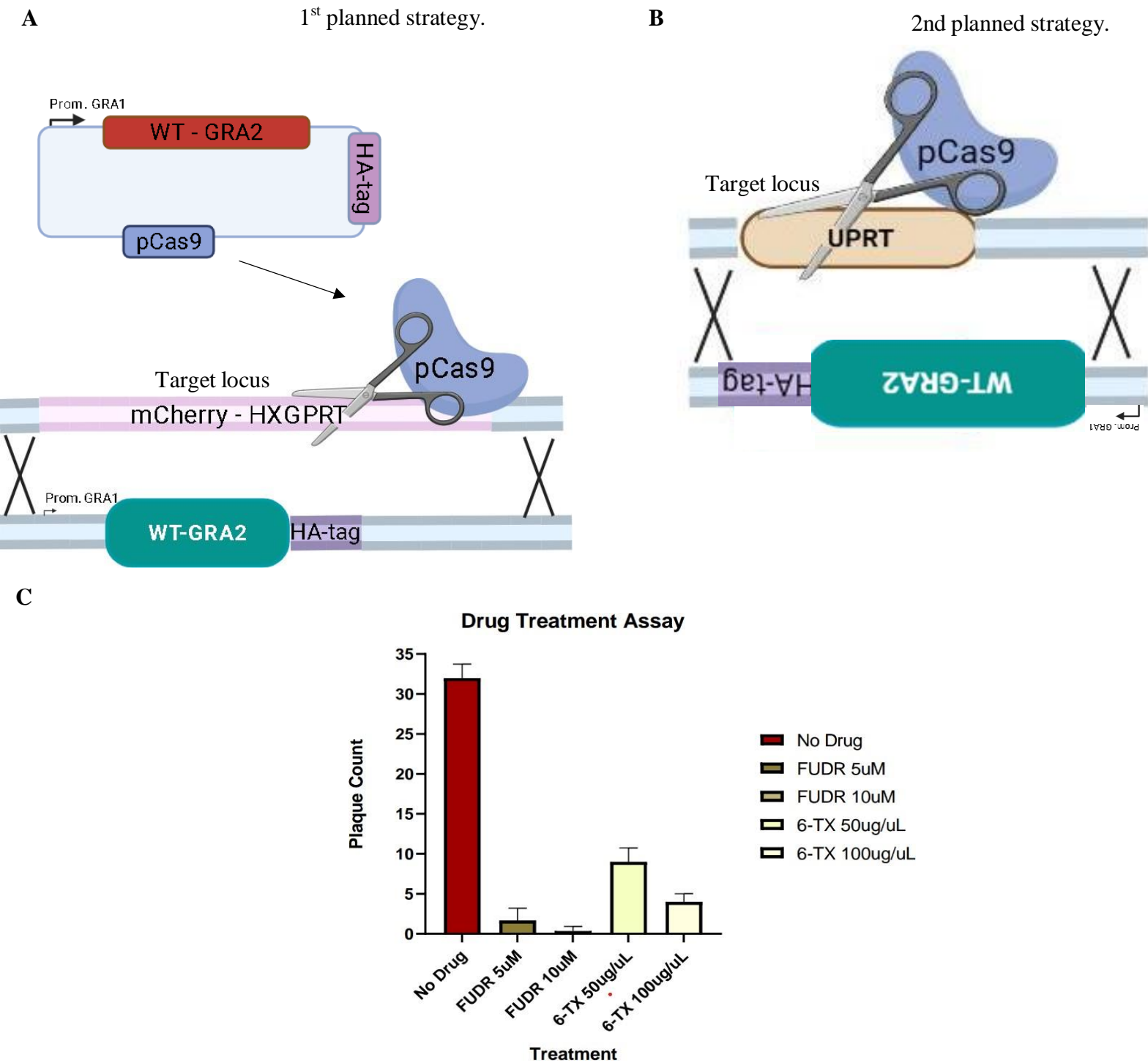
**Figure 1** Analysis of wildtype and desired phosphomutant GRA2 constructs (A) Structure of wildtype (red), phosphomimetic (blue) and phosphoablative (blue) GRA2. Domains are annotated to represent presence of amphipathic helix structures and residues that will be subject to SDM to create phosphomutants labelled on phosphomutant protein diagrams. (B) Amino acid translation of wildtype GRA2 protein with amphipathic helices (blue rectangles) marked under alignment of their predicted sequence. Helices are represented with helical wheels representing mutations falling within first amphipathic helix (S72 and S76) with their peak hydrophobic moment ( $\mu\text{H}$ ) and average hydrophathy (H) represented numerically, arrow pointing towards specific residues indicates where the peak hydrophobic moment falls within the sequence.

\*Highlights amino of interest for SDM, \* highlights amino acid changes following SDM to create phosphomutant GRA2

The first strategy of insertion aimed to restore GRA2 expression at the endogenous locus by amplifying our desired insert with arms of homology to  $\Delta$ GRA2 parasites. Previously completed lab work successfully created  $\Delta$ GRA2, involving the insertion of a KO locus (HXGPRT-mCherry). For our desired insertion, target of the *hxgpert* gene marker with pCas9 would allow for negative selection of parasites, using the drug 6-Thioxanthine (6-TX) (Fig 2A). However, it soon became apparent that this approach was ineffective, as mCherry expressing parasites were growing under this drug selection. Therefore, a different strategy was devised to target the *uprt* gene marker instead (Fig 2B) where Cas9 would cut, instead of *hxgpert*. Disruption of the *uprt* gene results in parasites that have resistance to 5'-fluoro-2'-deoxyuridine (FUDR) drug. The gene of interest would be inserted in an antisense orientation to increase transcription efficiency, supported by findings from (Bohne and Roos, 1997).

To observe the changes in strategy described above, we performed a drug treatment assay. Whereby we added 150 Me49 $\Delta$ ku80 parasites into triplicate wells containing different medias of the two drug treatments - 5 $\mu$ M and 10 $\mu$ M FUDR and 50 $\mu$ g/mL and 100 $\mu$ g/mL 6-TX. (Fig1D) shows the average plaque count of drug treated parasites. Considering the working concentration of 6-TX is 80 $\mu$ g/mL, when the 6-TX concentration was increased to 100 $\mu$ g/mL the parasites were able to form a greater number of plaques compared to the average plaque number of parasites in 5 $\mu$ M.

FUDR. FUDR when doubled in molarity (10 $\mu$ M) proved to be the most efficient at disrupting parasite growth. Hinting this 2<sup>nd</sup> strategy of using the plasmid (pCas9) targeting *uprt* and negative selection of (FUDR) is more suitable than that of targeting *hxgpert* and 6-TX drug treatment (Fig 2C). It must be stated that this data does contradict earlier transfection experiments conducted in our research group (data not shown).



**Figure 2** Comparing strategies for expressing HA-tagged GRA2 variants to complement  $\Delta$ GRA2 (A) First strategy of inserting GRA2 variants into the endogenous GRA2 locus, pCas9 plasmid targeting hxgprt gene (used to replace gra2 in KO generation) and GRA2-HA repair template in Me49ku80 $\Delta$ GRA2 parasites. Allowing 6-Thioxanthine (6-TX) drug for negative selection of successful transfectants (B) Second strategy of inserting GRA2-HA into uprt locus. pCas9 targeting uprt, co-transfected and linearized with repair template with homology to uprt UTR's. Allowing for 5'-fluoro-2'-deoxyuridine (FUDR) for negative selection of successful transfectants. (Figure depicts both strategies using WT-GRA2 as an example) (Cross linking (X) represents area of sequence homology, although are not representative of size) (C) Drug treatment assay using WT-Me49 $\Delta$ ku80 parasites in triplicate well plates exposed to two different concentrations of drug (FUDR and 6-TX). Parasites then allowed to plaque for 7 days before being fixed via 1% crystal violet staining and plaques counted. Shown are +SD of plaques in triplicate wells.

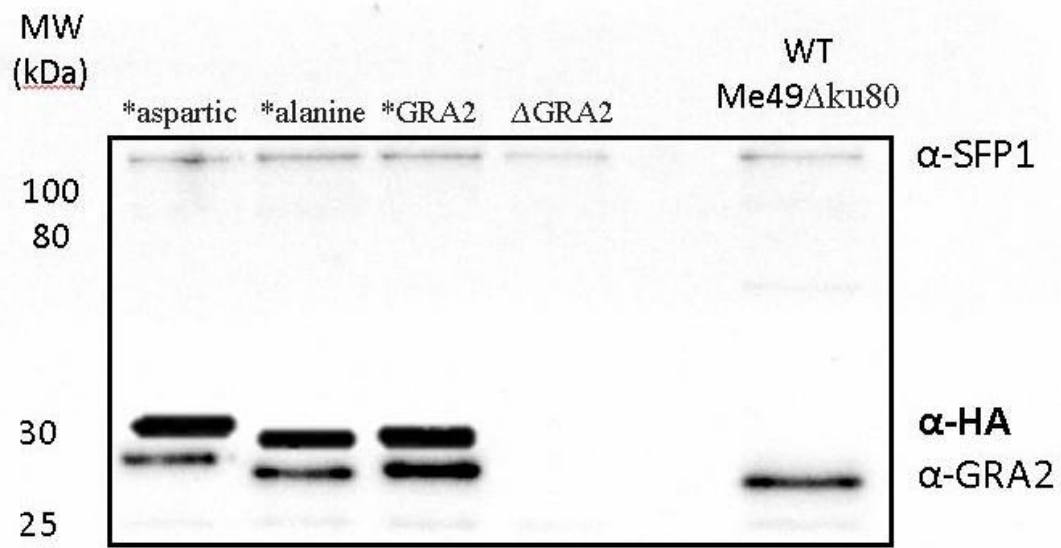
Upon validation of a successful method of parasite selection, we successfully carried out SDM of GRA2. This resulted in the creation of a phosphomimic GRA2 at residues 72 and 76 (GRA2\*aspartic) and phosphoablative GRA2 at residues 72 and 76 (GRA2\*alanine). We also wanted to complement a sequence of wildtype GRA2 (\*GRA2) into Me49 $\Delta$ ku80 $\Delta$ GRA2 parasite lines for comparison. To aid localization all transfected sequences were tagged with a single copy of the hemagglutinin epitope (HA). Following transfections of phosphomutant and wildtype GRA2 sequences into Me49 $\Delta$ ku80 $\Delta$ GRA2 parasites, we maintained a healthy infection in HFF's flasks. Gathering lysates from these flasks then allowed running of a Western Blot (Fig 3A),  $\Delta$ GRA2 and WT-Me49 $\Delta$ ku80 lysates were also ran for comparison. Probing of lysates was then conducted with antibodies targeting GRA2, HA and SFP1 (strand forming like protein 1) as a control.

Previous data describes the GRA2 protein as 25 kDa (Golkar et al., 2007), in lab work it is often seen to be slightly larger. This is due to post translational modifications following GRA2 secretion, and this finding is observed in our Western Blott (Fig 3A). Importantly the probing of antibodies helps to show that the complementation of the wildtype GRA2 as well as our phosphomutant sequences were successful. Although not precisely identical to the wildtype, the bands of our transfected GRA2 proteins show that it has been successfully inserted alongside the HA tag. The HA tag and phosphomutant GRA2 that contained the aspartic mutation at residues 72 and 76 seemed to show a slightly heavier molecular weight than the alanine mutation and WT GRA2.

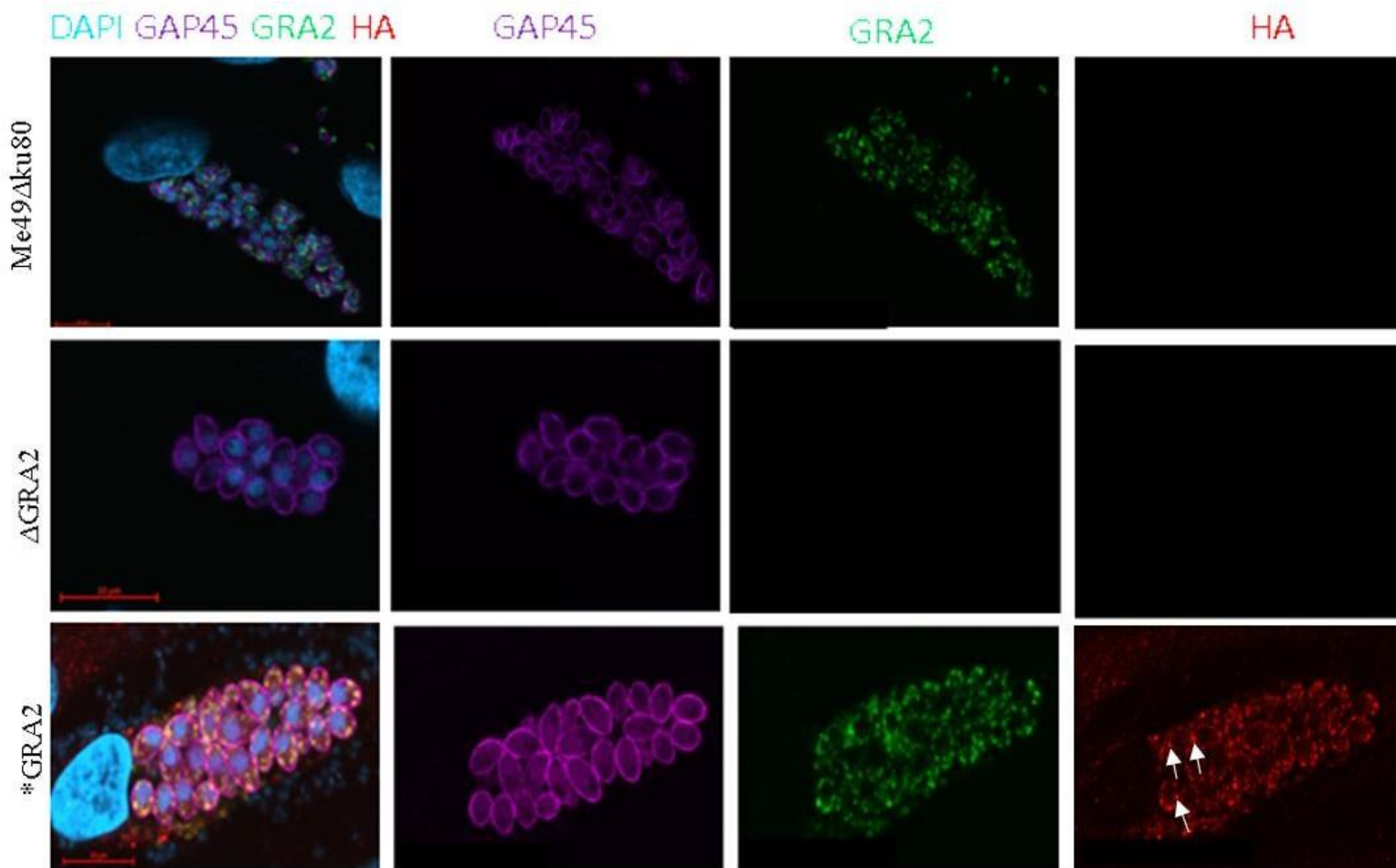
In order to visualize localization of complemented GRA2-HA (\*GRA2), monolayers of HFF's were infected with Me49 $\Delta$ ku80,  $\Delta$ GRA2 and \*GRA2 parasites. We wanted to view successful complementation in both stages, therefore we allowed

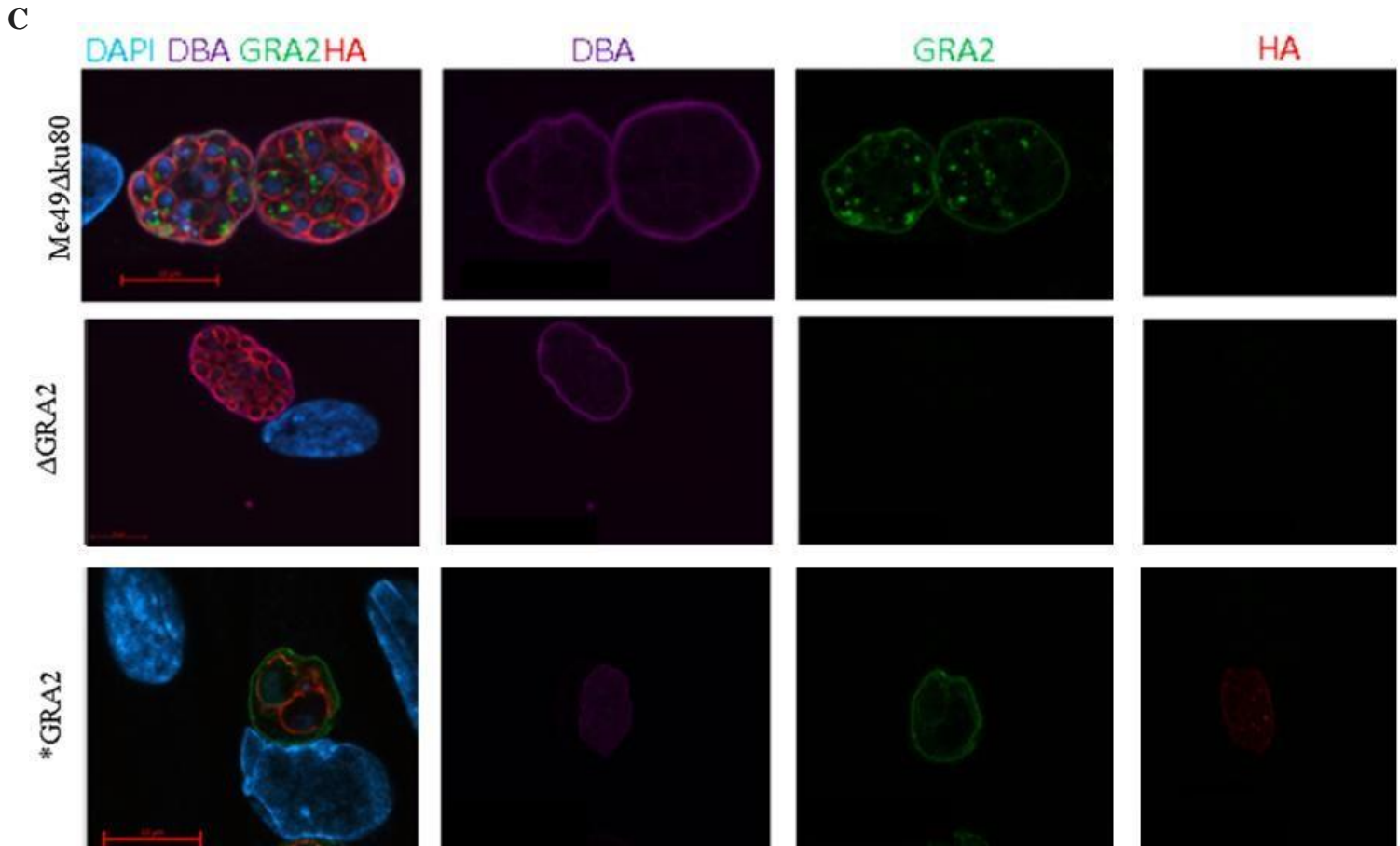
a 2-day incubation for tachyzoites and 7-day incubation for bradyzoite cultures. To assess GRA2 complementation we first probed tachyzoite samples with  $\alpha$ -HA,  $\alpha$ -GRA2 and  $\alpha$ -GAP45 antibodies. Whilst bradyzoite samples with an additional DBA staining to visualize the cyst wall (Fig 3B and C). These complementation's of GRA2-HA into Me49 $\Delta$ ku80 $\Delta$ GRA2 parasites were then examined with immunofluorescence microscopy. Whilst generally an overlap of signal was observed, it was discovered that  $\alpha$ -HA signal was generally poor. Importantly the signal from  $\alpha$ -GRA2 was stronger than  $\alpha$ -HA, with an increased background. We sought to observe GRA2 in its secreted state, our data unfortunately appears to show  $\alpha$ -HA tagged to GRA2 that is un-secreted (aided by white arrow in Fig 3B). Whilst in day 7 bradyzoites,  $\alpha$ -HA staining is also weak (Fig 3C). Due to these observations, in the subsequent phosphomutant experiments, it was decided to use  $\alpha$ -GRA2 instead of  $\alpha$ -HA as a reliable probing antibody to determine localization of GRA2. An alarming phenotype is also noticed in complementation of GRA2 in day 7 bradyzoites. Represented as a 'shrinking' of cysts with abnormal DBA signal in comparison to wildtype parasites. Phosphomutant GRA2 is not present in any these probed samples, indicating that this phenotype in mature cysts may be the result of targeted uprt genedisruption.

A



B

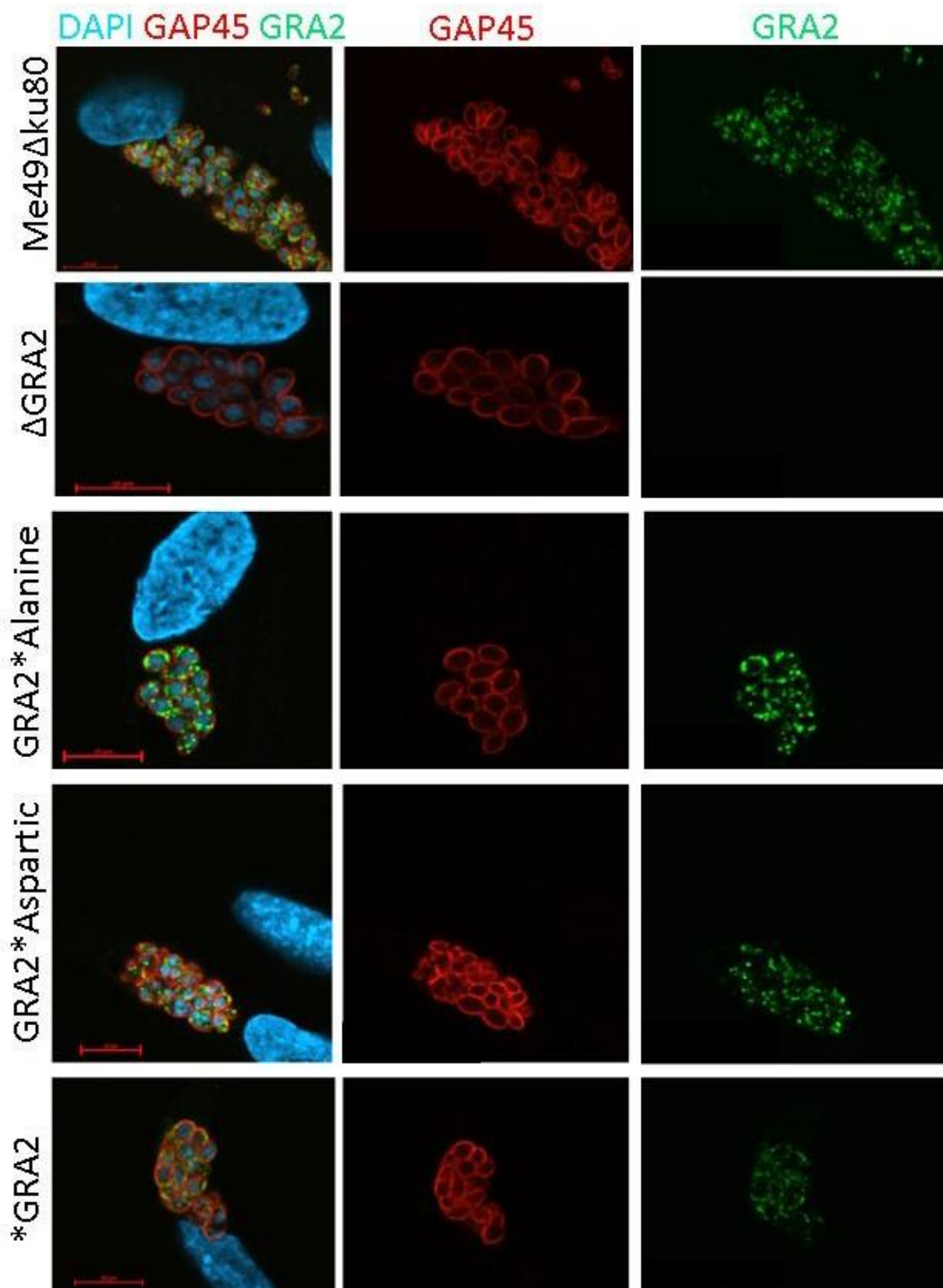




**Figure 3** Confirmation of WT and phosphomutant GRA2 transfection and poor  $\alpha$ -HA signal in tachyzoites and bradyzoites (A) Western blot analysis of lysates from infected HFFs with Me49 $\Delta$ ku80,  $\Delta$ GRA2, \*GRA2, GRA2\*72A+76A (\*alanine) and GRA2\*72D+76D (\*aspartic). Probed with anti-SFP1(1:2000), anti-GRA2 (1:1000) and anti-HA (1:1000) antibodies, then with anti-rabbit (1:10000), anti-mouse (1:1000) and anti-rat antibodies (1:5000). \*Indicates a transfected with mutant or complemented GRA2-HA. (B) Immunofluorescence analysis of day 2 tachyzoite HFF's infected with Me49 $\Delta$ ku80,  $\Delta$ GRA2, \*GRA2. Red, anti-HA; Green, anti-GRA2. Purple, anti-GAP45 Blue, DAPI. White arrows indicate HA tagged to un-secreted GRA2. (C) Immunofluorescence analysis of day 7 bradyzoite infected HFF's with Me49 $\Delta$ ku80,  $\Delta$ GRA2, \*GRA2. Red, anti-HA; Green, anti-GRA2. Purple, DBA to stain the cyst wall; Blue, DAPI. All scale bars represent 10 $\mu$ M.

In order to visualize localization of phosphomutant GRA2 in tachyzoites (GRA2\*Alanine and GRA2\*Aspartic), monolayers of HFF's were infected with Me49 $\Delta$ ku80,  $\Delta$ GRA2, GRA2\*Alanine, GRA2\*Aspartic and \*GRA2 parasites. These infected monolayers were incubated for 2 days in tachyzoite conditions. Antibody probing of samples was conducted with  $\alpha$ -GRA2 and  $\alpha$ -GAP45 antibodies. Following this, immunofluorescence microscopy was conducted, aiming to observe the localization of phosphomutant GRA2, specifically if mutations to phosphosites (S72 and S76) could affect GRA 2 movement.

(Fig 4A) shows that during the tachyzoite stage, parasites expressing phosphomimetic GRA2 (GRA2 \*Aspartic) does not influence protein localization within the PV. Observed as puncta in the PV and spread equally across the vacuole. Phosphoablative GRA2 (GRA2 \*Alanine) also appears to show a similar pattern of localization. Both findings support previous literature (Guevara et al., 2019) indicating that GRA2 is secreted by the parasite after PV formation. The structure of the PV is also normal in shape. The localization of GRA2 here show both phosphomutants in tachyzoites are unable to affect its movements.

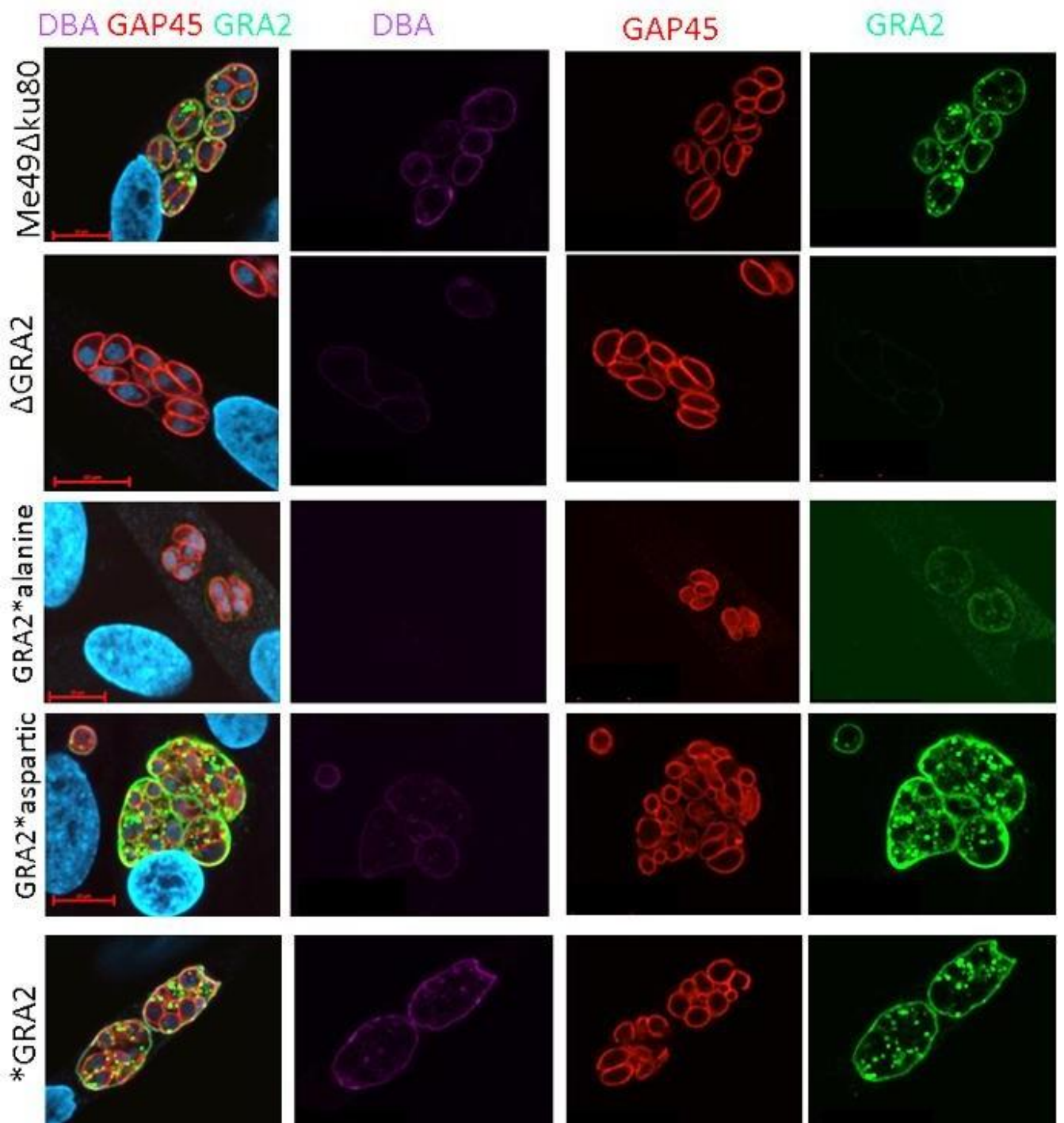


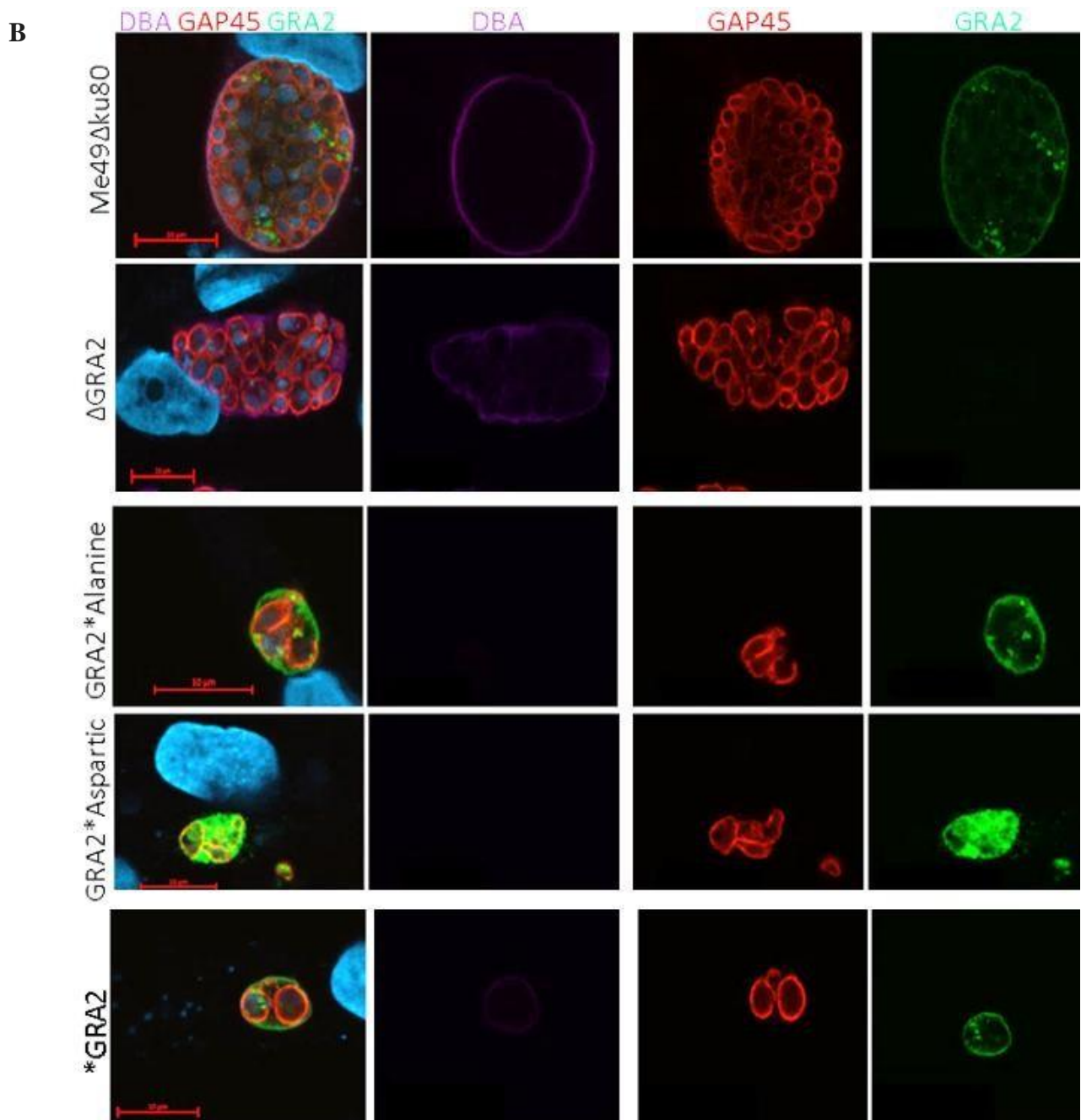
**Figure 4** Phosphomutant GRA2 in tachyzoites has little effect on localization in PV (A) Immunofluorescence analysis of day 2 tachyzoite HFF's infected with Me49 $\Delta$ ku80,  $\Delta$ GRA2, GRA2\*aspartic, GRA2\*alanine and \*GRA2. Red, GAP45; Green, anti-GRA2; Blue, DAPI.

With a lack of phenotype observed in response to phosphomutant GRA2 in tachyzoites, we continued our investigation now examining phosphorylation in chronic infection. Monolayers of HFF's were infected with Me49 $\Delta$ ku80,  $\Delta$ GRA2, GRA2\*Alanine, GRA2\*Aspartic and \*GRA2 parasites. These infected cells were left to incubate in bradyzoite conditions for 2 and 7 days, respectively. In addition to probing bradyzoite samples with  $\alpha$ -GAP45 and  $\alpha$ -GRA2 antibodies, we used DBA staining, to visualize any effects on cyst wall structure and CST1.

In day 2 bradyzoites, a weak signal of  $\alpha$ -GRA2 is noticed in phosphoablative GRA2 (Fig 5A). Additionally, an absence of DBA staining is seen here, suggesting that phosphoablative GRA2 shows a reduced level of colocalized CST1 in day 2 bradyzoites. In phosphomimetic GRA2, we can see a normal level of  $\alpha$ -GRA2 staining at the cyst wall as well as puncta in the matrix. Additionally, DBA signal is more readily observed in these cysts. In mature, day 7 cysts, targeting of the *uprt* gene marker appears to be detrimental to cyst size and structure in both phosphomutants (Fig 4C). Repeat observation of complemented GRA2-HA also resulted in observing a 'shrunk' cyst phenotype and irregular DBA staining, confirming our initial findings (Fig 3C). Due to abnormal cyst size and shape as a result of *uprt* gene disruption, it is impossible to infer a relationship between phosphomutant GRA2 and CST1 here. Taken together, such findings indicates that for mature cyst growth, different methods of gene marker selection and/or bradyzoite differentiation be tested and researched.

A





**Figure 5** Targeting of *uprt* gene marker in creation of phosphomutants leads to abnormal ‘shrunk’ mature cysts (A)

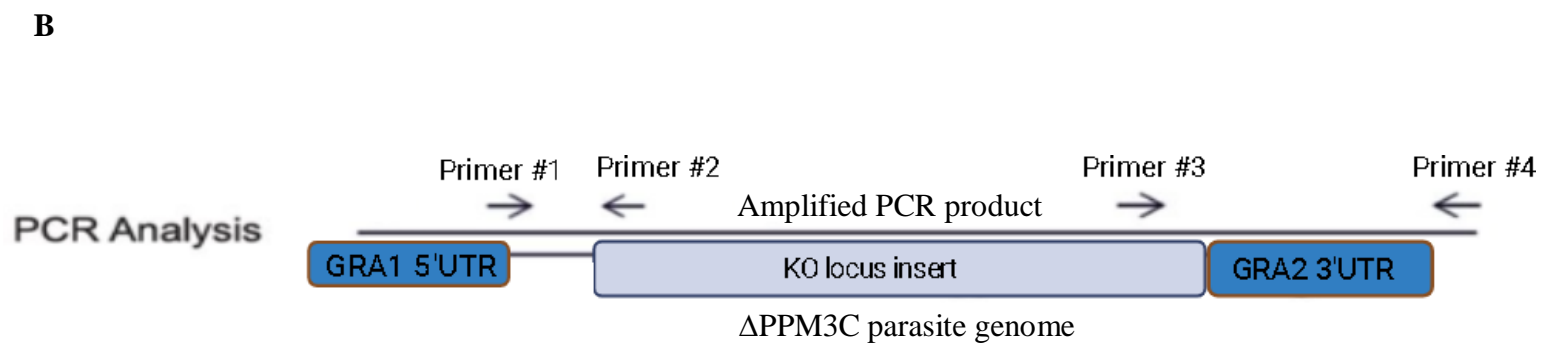
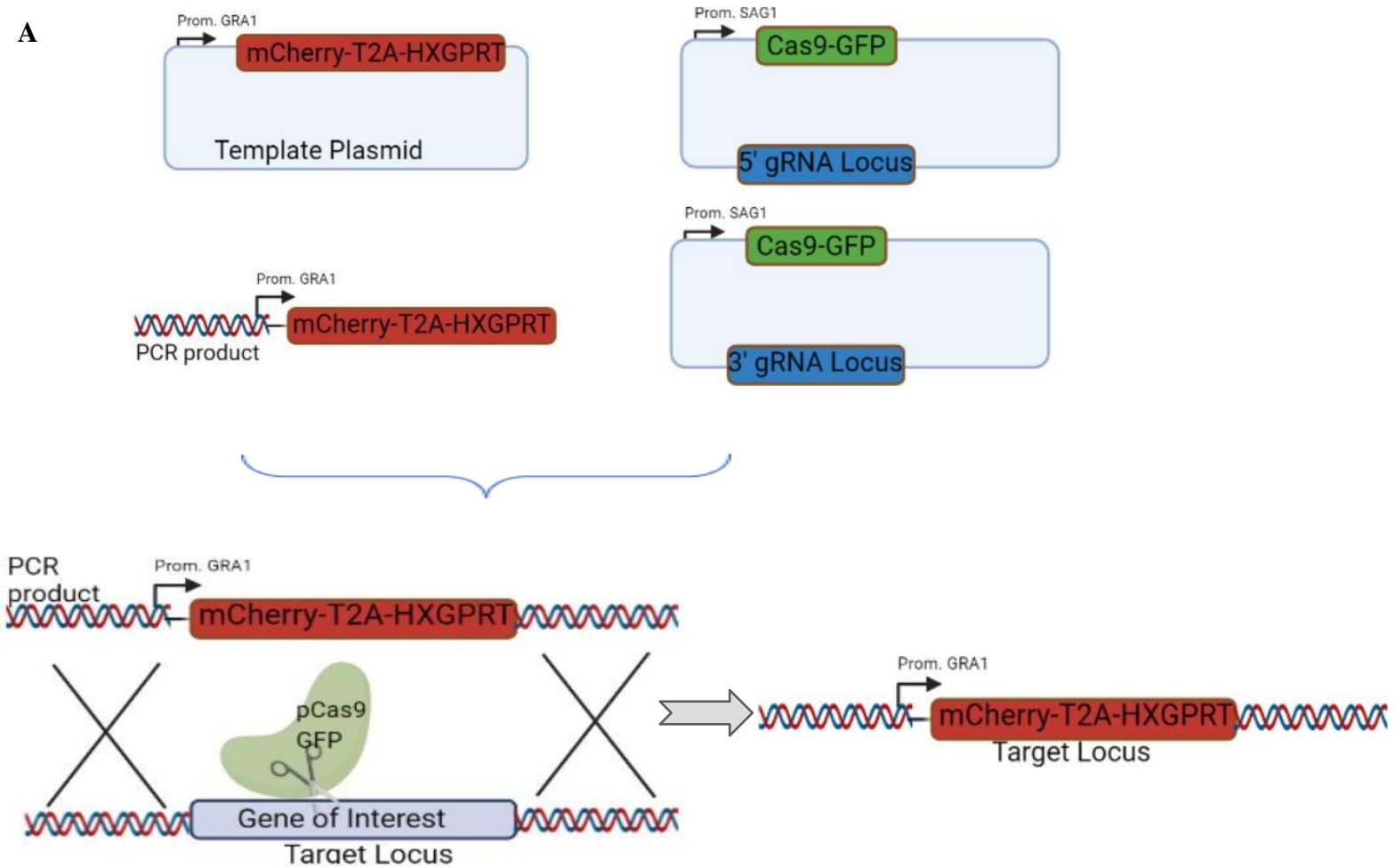
Immunofluorescence analysis of day 2 bradyzoite and (B) day 7 bradyzoite infected HFF’s with Me49 $\Delta$ ku80,  $\Delta$ GRA2, GRA2\*aspartic, GRA2\*alanine and \*GRA2. Green, anti-GRA2; Purple, DBA to stain the cyst wall; Red, GAP45; Blue, DAPI. All scale bars represent 10 $\mu$ M. \*indicates compliment or phosphomutant GRA2.

$\Delta$ PPM3C cultures have previously been created in previous research (Mayoral et al., 2020), and showed that parasites had a loss of virulence *in vivo*. Conclusions were drawn that this was due to the importance of PPM3C in regulating secreted proteins. A relationship was hypothesized with GRA2, as a marked increase of GRA2 phosphopeptides found in  $\Delta$ PPM3C parasite cultures. However, they were unable to find dysregulated GRA2 within tachyzoite PV's, at 32 hours post infection. Dysregulation of GRA2 could indeed occur at a later timepoint, in tachyzoites as well as in cyst development. Addressing this we wanted to create  $\Delta$ PPM3C parasites, with the aim of investigating the movement of GRA2 at later points in infection.

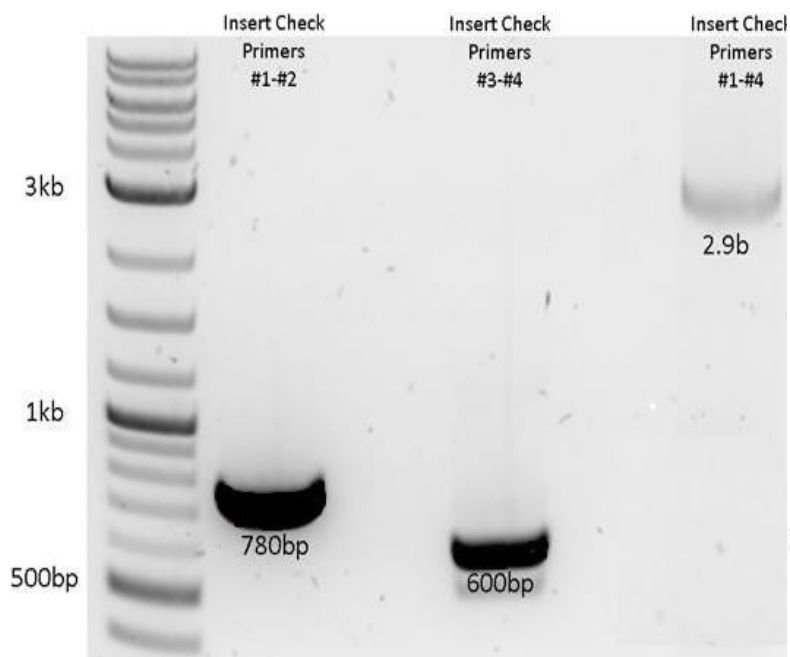
Our strategy to create  $\Delta$ PPM3C first involved the cloning of 5' and 3' gRNA targeting PPM3C into the plasmid backbone of Cas9-GFP (primers listed in Table S1). Alongside this we amplified an mCherry-HXGPRT repair template. Transfection occurred in Me49 $\Delta$ ku80 $\Delta$ HXGPRT parasites, following the combination of the 5' and 3' gRNA Cas9-GFP plasmids and the mCherry-HXGPRT construct, leaving our desired knockout locus in place (Fig 6A). This approach was also used in order to attempt creation of  $\Delta$ PPM3A parasites, unfortunately following transfection, a healthy infection of parasites was not seen. It was decided that future experiments focused solely with  $\Delta$ PPM3C parasites.

Once  $\Delta$ PPM3C parasite lines had been successfully cultured leading to a healthy infection within HFF flasks. They were subject to single cell cloning with two suspected  $\Delta$ PPM3C isolated clones grown. Insertion check primers (listed in Table S1) were then used in order to confirm correct mCherry-HXGPRT insertion as our desired KO locus (Fig 6B). Primers #1-#4 amplify the entire fragment of KO insert (mCherry-HXGPRT) measuring ~3kb. Primers #1-#2, #3-#4 resulted in a smaller amplification of fragments of ~800bp and ~600bp respectively.

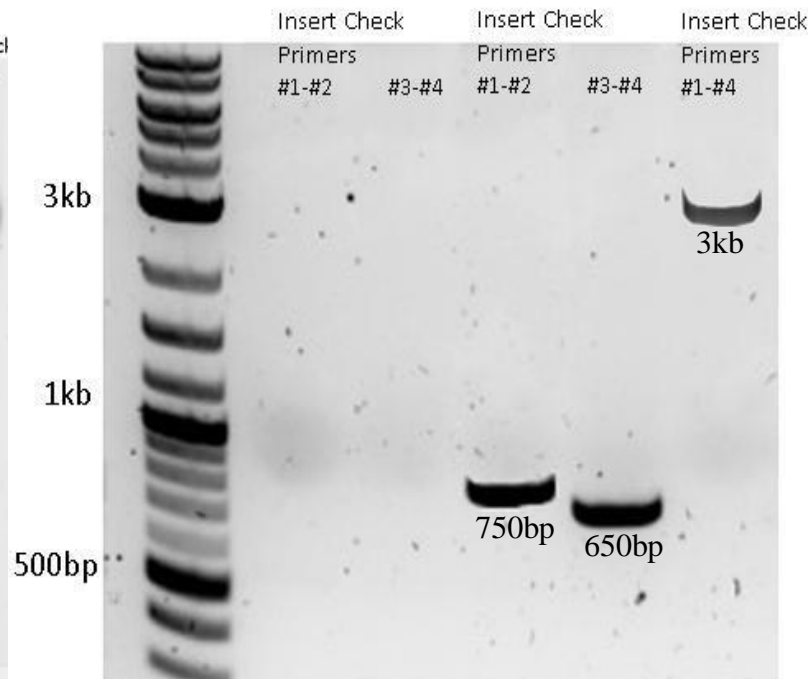
(Fig 6C) shows a gel with probed gDNA from a population flask of  $\Delta$ PPM3C confirming proper insertion of mCherry-HXGPRT. A large fragment amplifying the entire KO locus as well as smaller fragments including regions of homology to the parasite genome are seen. (Fig 6D) images a gel containing gDNA of isolated clone 1 that was probed with same insertion check primers. This additionally confirmed our desired KO locus, with WT gDNA from Me49 $\Delta$ ku80 $\Delta$ HXGPRT showing no amplification for the insertion check primers. Clone 2 (data not shown) could not be confirmed to contain our desired KO locus.



C

 $\Delta$ PPM3C Population

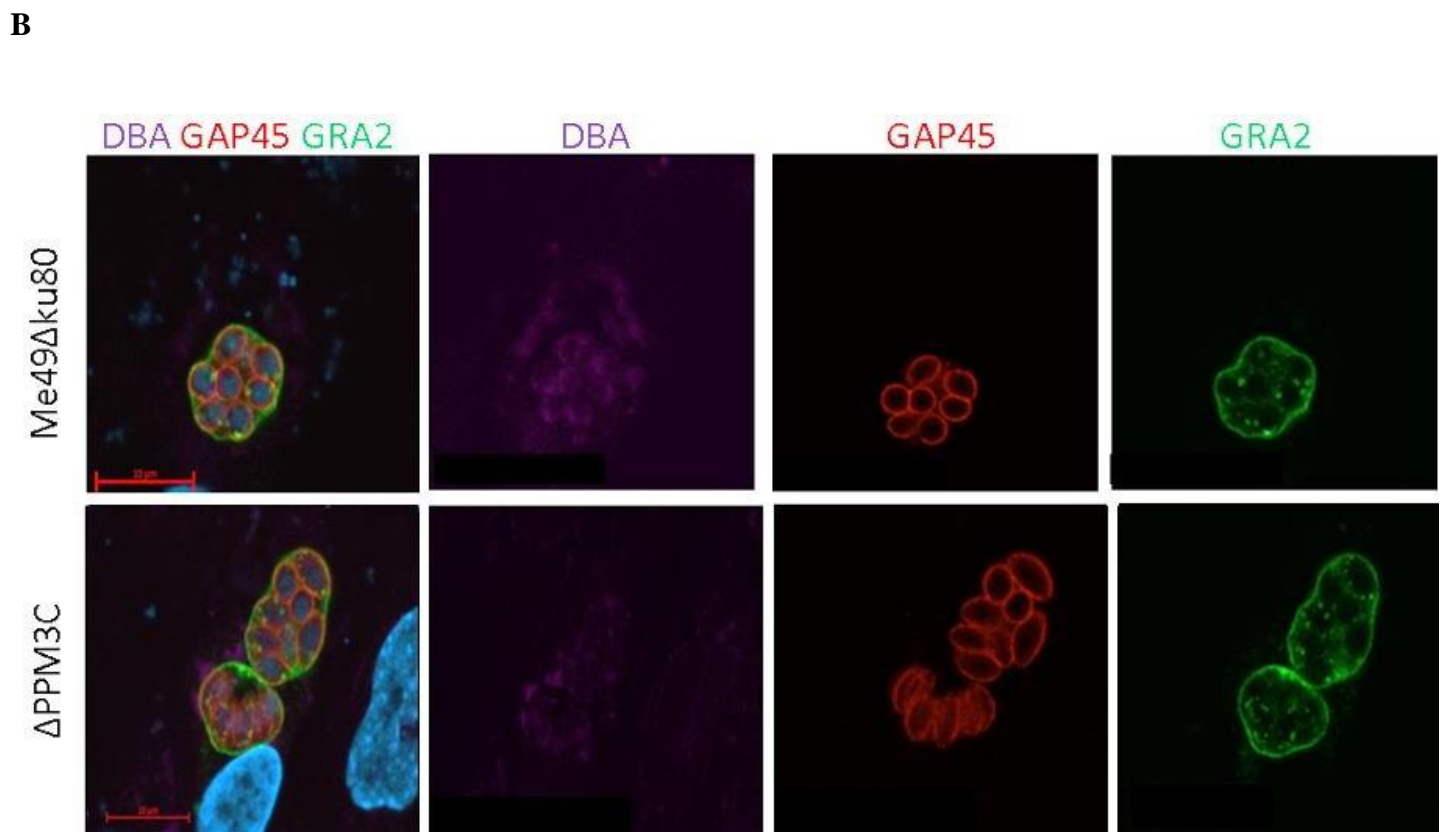
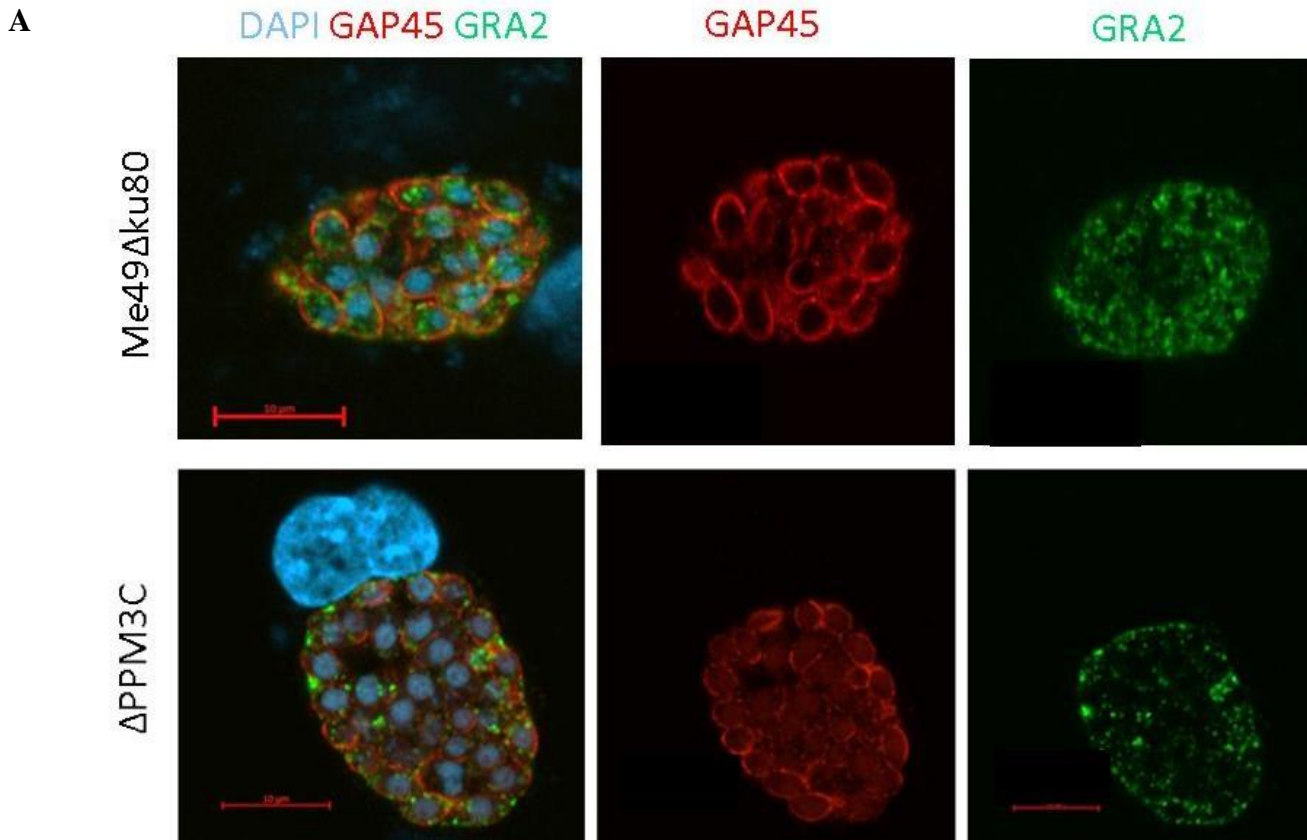
D

Me49 $\Delta$ ku80 $\Delta$ PPM3C Clone 1

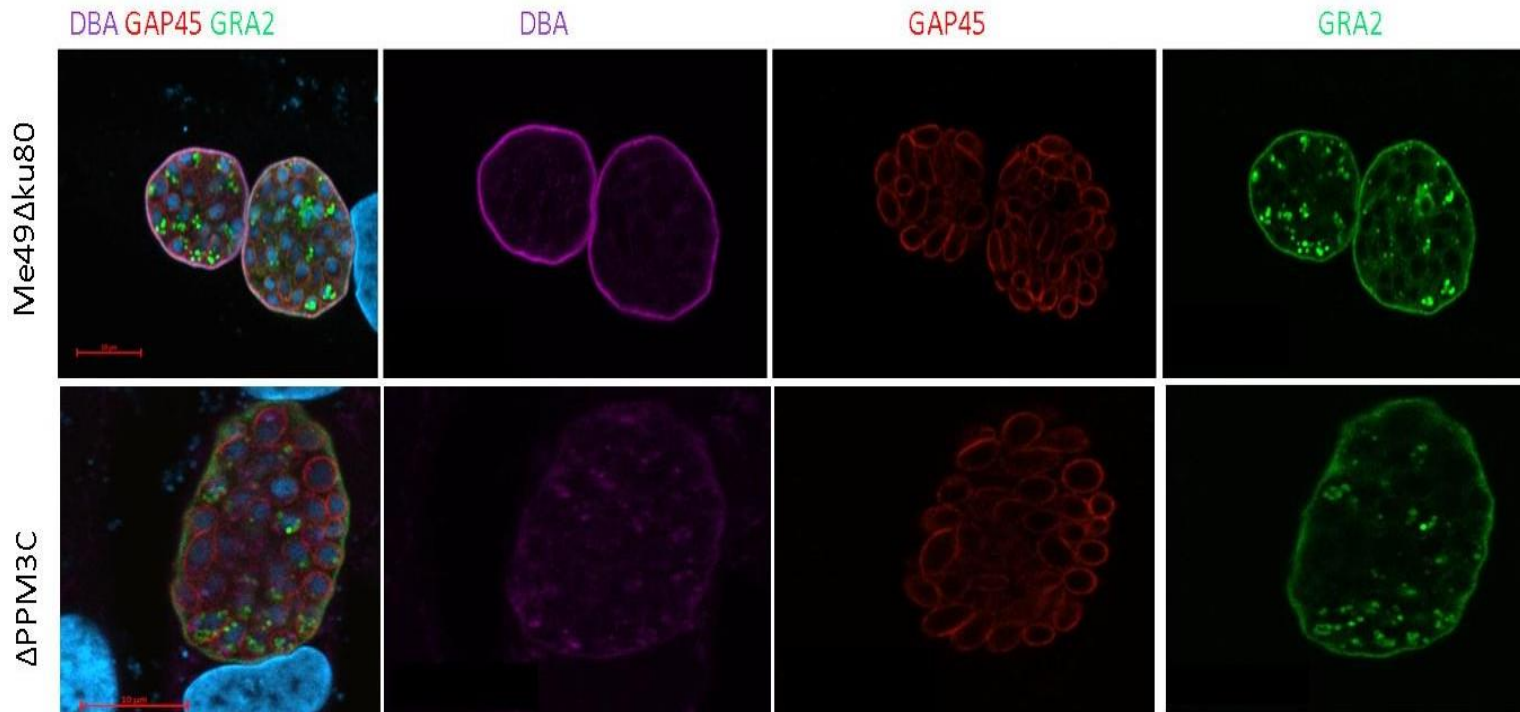
**Figure 6** Creation of  $\Delta$ PPM3C (A) Strategy of creating  $\Delta$ PPM3C locus via amplification of mCherry – HXGPRT and combining of pCas9 5' and 3' gRNA plasmids targeting HXGPRT in Me49 $\Delta$ ku80 $\Delta$ HXGPRT parasites. (B) diagram to represent the amplification of insertion check primers (listed in Table S1) to probe and confirm correct KO locus insertion in population and isolated clones of  $\Delta$ PPM3C. (C) 1% gel agarose to show confirmation of  $\Delta$ PPM3C probing population template with primers designed to check proper insertion of mCherry – HXGPRT. (D) 1% gel agarose confirming correct insertion of desired KO locus probing Me49 $\Delta$ ku80 in lanes 1-2 and  $\Delta$ PPM3C Clone 1 in lanes 3-5. Lanes are headed by labels describing insert primers that are used to probe template from population and isolated clone 1 of  $\Delta$ PPM3C.

To view the effect of  $\Delta$ PPM3C on GRA2 we infected 12 well plates that contained HFF's grown on coverslips. These were then infected with  $1 \times 10^5$  parasites of Me49 $\Delta$ ku80 $\Delta$ PPM3C parasites. Viewing 3 different time points, we had 2 plates that were left to incubate for 2 days at tachyzoite and bradyzoite conditions. Whilst 1 plate was left to incubate for 7 days at bradyzoite conditions. Following this came antibody probing with  $\alpha$ -GAP45,  $\alpha$ -GRA2 in tachyzoites. Bradyzoites were additionally probed with DBA to visualize the cyst wall. The following images were then produced with immunofluorescence microscopy.

A general comment here, specifically regarding the insert of mCherry into the KO locus of our parasites. It was observed during microscopy that signal from  $\alpha$ -GAP45 was superior to that from mCherry. If another channel was used to visualize  $\alpha$ -GAP45, red signal would have been observed due to presence of mCherry in  $\Delta$ PPM3C parasites. (Fig 6A) shows at day 2 of tachyzoite conditions, there is a slight reduction in  $\alpha$ -GRA2 signal in the PV compared to the wildtype. Specifically, localization is more concentrated towards the PVM rather than the PV space. Day 2 of bradyzoite growth shows  $\Delta$ PPM3C parasites appear to have no significant effect on GRA2 localization in comparison to wildtype cysts. Wildtype and  $\Delta$ PPM3C cysts exhibited GRA2 movement as proposed in the model by (Guevara, Fox and Bzik, 2020). Such a model outlines that GRA2 is located within cyst matrix as well as equally towards the cyst wall in day 2 bradyzoites. The key finding is seen in day 7  $\Delta$ PPM3C cysts, where DBA staining is clearly deficient at the cyst wall (Fig 6C). This finding was observed in repeated stains of DBA in other day 7  $\Delta$ PPM3C bradyzoites (images not shown). Taken together, these preliminary findings show that  $\Delta$ PPM3C mature cysts, have a reduced localization of CST1 at the cyst wall.



C



**Figure 7** Preliminary results  $\Delta$ PPM3C leads to a decrease of CST1 in cyst wall in mature cysts but minimal impact on GRA2 in tachyzoites (A) Immunofluorescence analysis of day 2 tachyzoite infected HFF's with Me49 $\Delta$ ku80 $\Delta$ PPM3C and WT - Me49 $\Delta$ ku80 parasites. Green, anti-GRA2; Red, anti-GAP45 and DAPI (B) Immunofluorescence analysis of day 2 Bradyzoite infected HFF's with Me49 $\Delta$ ku80 $\Delta$ PPM3C and WT - Me49 $\Delta$ ku80 parasites. Purple, DBA to stain the cyst wall; Green, anti-GRA2; Red, anti-GAP45 and DAPI (C) Immunofluorescence analysis of day 7 Bradyzoite infected HFF's with Me49 $\Delta$ ku80 $\Delta$ PPM3C and WT - Me49 $\Delta$ ku80 parasites. Purple, DBA to stain the cyst wall; Green, anti-GRA2; Red, anti-GAP45 and DAPI. All scale bars represent 10 $\mu$ M.

Previous work in the lab created genetic knockout parasite strains of  $\Delta$ CST1,  $\Delta$ GRA2 and  $\Delta$ CLP1. In order to assess cyst durability after biochemical degradation we designed a first experiment involving acid pepsin digestion. This included 3 parasite lines – Me49 $\Delta$ ku80,  $\Delta$ GRA2 and  $\Delta$ CST1. A population of parasites from each of the parasite lines were subject to no digestion of acid pepsin – 0 minutes. Previous lab work (unpublished data) showed that wildtype tachyzoites, after 5 minutes of digestion were killed. As a result, we used a 5-minute incubation period as a means of killing residual tachyzoites within bradyzoite populations. Theoretically, this would allow us to confidently compare against a 10-minute incubation of acid pepsin digestion. The neutralization of the acid pepsin solution was performed after the respective acid pepsin incubations, with the use of  $\text{Na}_2\text{CO}_3$ . 150 parasites were then seeded into duplicate wells to allow for plaque growth. A 1% Crystal Violet (CV) fixing and staining method was used, after which light microscopy allowed manual counting of plaque numbers.

(Fig 8A) shows the mean plaque count of these wells and parasite lines according to length of time that the bradyzoites were exposed to acid pepsin digestion. Graph (Fig 8C) plots these average plaque counts.  $\Delta$ CST1 parasites, suffering from the loss of the critical cyst wall protein, expectedly saw loss of plaque formation. 5 minutes incubation with acid pepsin is deemed enough to either kill bradyzoites held within cysts, in their weakened structure. With no plaques observed in the 10-minute wells containing  $\Delta$ CST1 parasites, and very few on average (4) in the 0-minute wells.  $\Delta$ GRA2 appeared to also suffer a loss in plaquing ability when exposed to acid pepsin digestion with a small average number counted in the 5- and 10-minute wells (5 and 4 respectively). At 0 minutes exposure  $\Delta$ GRA2 parasites

were seen to form plaques at a much larger number, likely this is due to the residual tachyzoites that were within the population.

These findings led to a review of the protocol and a second repeated experiment. (Fig 8B) shows this repeated plaque assay with the inclusion of another parasite line,  $\Delta$ CLP (Chitinase-like protein 1). Chitin is a form of  $\beta$  (1-4) N-acetyl-D-glucosamine, in *Toxoplasma*, first discovered during the transition stage between tachyzoite and bradyzoite (Almeida et al., 2015). To detect the presence of Chitin, (Boothroyd et al., 1997) showed that wheat germ agglutinin (WGA) can bind at the cyst wall. Treatment of the cysts with artificial chitinases led to a phenotype of failure to bind WGA as well as bradyzoite release from the cyst. (Almeida et al., 2015) confirmed the presence of CLP1 as one secreted chitinase that was secreted by the parasite. Preliminary evidence (Conference Presentation 2022, unpublished data) discussed that deletion of CLP1 may lead to an increase in plaque growth due to the release of bradyzoites in cysts.

With this in mind, we supplemented our experiment with  $\Delta$ CLP parasites to assay with pepsin digestion. (Fig 8C/D) confirms that loss of the CLP1 resulted in an increased number of plaques, once bradyzoites were released from the cyst wall structure. After 5 minutes of acid pepsin digestion, the average plaque number counted (30) was higher than that of the Me49 $\Delta$ ku80 (17). After 10 minutes of pepsin digestion, the  $\Delta$ CLP average plaque count (10) was much lower. Indicating that 10 minutes of incubation may have been enough to kill almost two thirds of the parasites.  $\Delta$ CLP plaque counts were additionally higher than both other gene knockout parasites,  $\Delta$ CST1 and  $\Delta$ GRA2, with only 1 plaque on average counted after 10 minute of digestion. However, both  $\Delta$ CST1 and  $\Delta$ GRA2 in the repeat experiment show no plaque growth after 0-minute incubations, in comparison to the first

experiment where plaque growth was seen. The 0-minute digestions of the Me49 $\Delta$ ku80 (both repeats) with low levels of mean plaque counts (6 and 8) suggest that with no exposure to biochemical stress, bradyzoites can still spontaneously differentiate and infect neighboring cells.

Due to inconsistent results seen in both experiments, it was decided to halt repeat experiments. Namely so that a review of the protocol could be carried out to obtain a more reliable and quantifiable source of data.

A

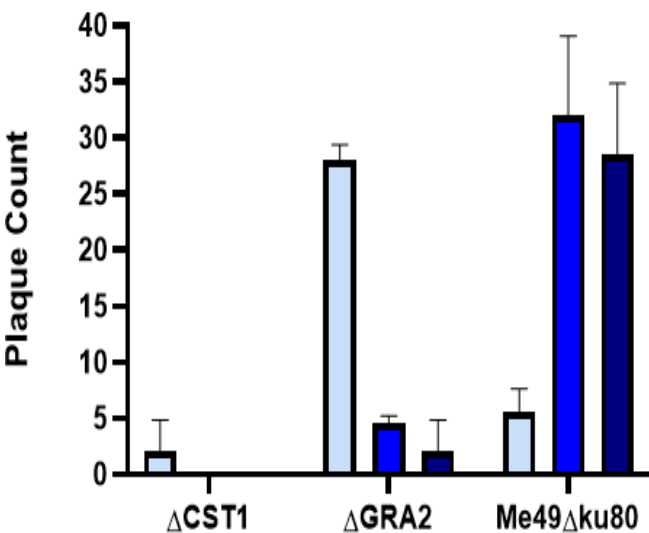
Parasite Line	0 Minutes	5 Minutes	10 Minutes
Me49 $\Delta$ ku80	6	32	29
$\Delta$ GRA2	28	5	4
$\Delta$ CST1	4	0	0

B

Parasite Line	0 Minutes	5 Minutes	10 Minutes
Me49 $\Delta$ ku80	8	20	30
$\Delta$ GRA2	0	6	1
$\Delta$ CST1	0	2	1
$\Delta$ CLP1	2	30	10

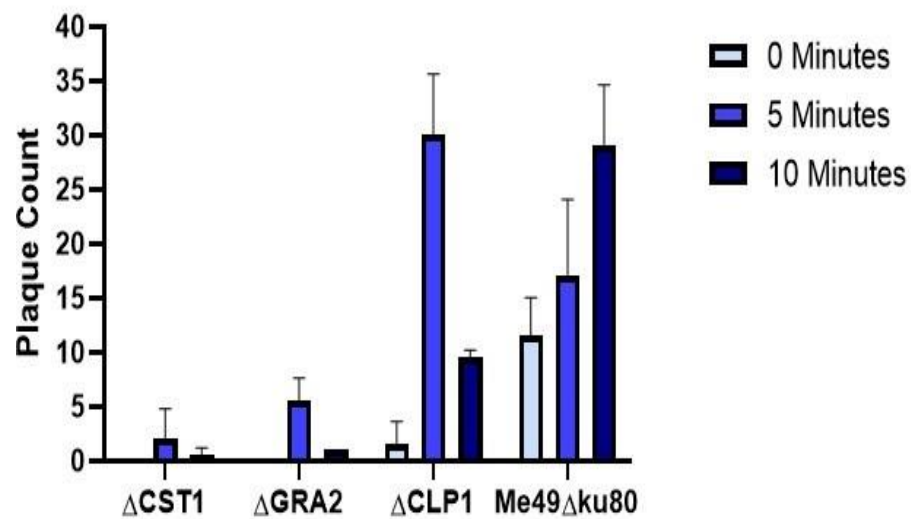
C

## Pepsin Treatment Plaque Assay 1



D

## Pepsin Treatment Plaque Assay 2



**Figure 8** Plaque assay comparing gene deletion and wildtype parasites after acid digestion. (A) Me49 $\Delta$ ku80,  $\Delta$ GRA2 and  $\Delta$ CST1 - mean plaque counts from well plates that contained bradyzoites exposed to 0,5- and 10-minute length incubations of acid pepsin digestion before allowed to form plaques. 1% crystal violet staining used to fix, and manual counting performed under light microscopy. (B) mean plaque count performed with same experimental conditions as first experiment with supplemented  $\Delta$ CLP1 parasite line (C) Graph of mean plaque count from experiment one (D) Graph of mean plaque count from repeat experiment with supplemental  $\Delta$ CLP1 parasite line, shown are +SD of plaques in duplicate wells.

## Discussion

During the course of this investigation, we wanted to examine phosphoregulation in *Toxoplasma Gondii*. Specifically in the secreted GRA2 protein and phosphatase, PPM3C. Overall, we were unable to illustrate the chronic regulation of GRA2 in *Toxoplasma Gondii*. This was due to an abnormal cyst phenotype, due to *uprt* gene disruption in day 7 bradyzoites. Our preliminary results regarding  $\Delta$ PPM3C show little impact on GRA2, however they infer that this gene deletion leads to a reduction of CST1 at the cyst wall periphery.

### Initial CST1 Problem

After moving on from working with CST1, our results regarding gene deletion of PPM3C support its discussion here. Our work was designed on expressing the protein in tachyzoites to monitor any potential movement here. Successful PCR amplification from wildtype parasite was followed by unsuccessful repeat attempts to insert it into a plasmid backbone. Due to limited resources and time constraints, it was decided to move on with research regarding phosphomutant GRA2 and PPM3C. It is well established that CST1 is upregulated in bradyzoites (Tomita et al., 2013), although our attempt to express it in tachyzoites was unsuccessful. It remains a future avenue of research to pursue, as this could detail previously undescribed movements of CST1 in tachyzoites.

### Poor $\alpha$ -HA signal

GRA2 complementation (Fig 3 B, C) shows a poor  $\alpha$ -HA signal given from our complimented GRA2 attempts. In tachyzoites,  $\alpha$ -HA signal does overlap with  $\alpha$ -GRA2, however the coverage is not completely aligned with  $\alpha$ -GRA2. Whilst in

mature bradyzoites, the signal is additionally quite weak in comparison to  $\alpha$ -GRA2, in the complemented GRA2 line. This is unfortunate as the HA epitope was strategically added to our phosphomutant and indeed wildtype GRA2 so that transfection could be localized, once expressed. Signal given from  $\alpha$ -GRA2 was far superior in both tachyzoite and bradyzoites and importantly would allow visualization of GRA2 once secreted. It was discussed that the epitope once bound to  $\alpha$ -HA could behave in a different manner once secreted by the parasite, leading to poor binding with the antibody. Perhaps this begins to reason the incomplete signaling pattern observed in the PV, as it appears the  $\alpha$ -HA signal is bound to GRA2 that is not yet secreted by the parasite. Once GRA2 is secreted by the parasite into the space of the PV, it is possible the orientation of the epitope and conditions that require proper binding to  $\alpha$ -HA are changed – leading to poor signal. A potential point of improvement regarding poor staining of  $\alpha$ -HA could be the use of Saponin during permeabilization of tachyzoite samples. Our current method was to permeabilize tachyzoites for 2 minutes with 0.1% PBS-T. The tachyzoite PVM acts as a protective layer for *Toxoplasma Gondii* (Paredes-Santos et al., 2019). Certainly, it is possible that our method of permeabilization is inefficient in allowing sufficient antibody-target binding. Saponin can form pores in membranes of cells without destroying them entirely (Jacob, Favre and Bensa, 1991). It is also considered a mild method of permeabilization in comparison to reagents such as Triton-X100 Scheffler (Schiefermeier and Huber, 2014). Milder forms of permeabilization may aid in preservation of antigenic epitope orientations, this could also rectify an issue we hypothesize occurred in our experiments. Protocols vary in its usage from 0.2%-5%, 10-30 minutes ([abCam-fixation and permeabilization in IHC/ICC](#)). Usage of Saponin

as a permeabilization technique should undoubtedly be implemented into the protocol of future experiments and immunofluorescence microscopy.

### Uprt Gene Disruption and Bradyzoite Differentiation

Our first set of experiments with GRA2 discuss the initial process of inserting WT and phosphomutant GRA2 via replacing of the endogenous KO locus in Me49 $\Delta$ ku80 $\Delta$ GRA2. This was initially strategized via targeting of the *hxgprrt* gene marker (Fig 2A). However, this proved to be ineffective following the subsequent drug treatment of 6-TX, at the working concentration of 80 $\mu$ g/mL. Initially observed in the cultured flasks of HFF's with numerous parasites expressing mCherry signal, more-so than expected. To propose a new strategy, we discarded targeting of the endogenous locus and moved towards a new strategy of phosphomutant and complemented GRA2 insertion into the *Toxoplasma*. This involved pCas9 targeting the *uprt* gene marker in the parasite genome (Fig 2B). Disruption of this gene marker allowed for drug treatment with FUDR at 5 $\mu$ M and was observed to efficient at killing more parasites whilst still leaving a healthy infection in HFF flasks. Conducting a drug assay comparing the two drug treatments with 2 different concentrations/molarity concluded that FUDR was more efficient at killing parasites than 6-TX (Fig 2C). These encouraging results further supported the strategy to insert WT and phosphomutant GRA2 targeting the *uprt* gene marker. Uracil phosphoribosyl transferase (*uprt*) is a gene that encodes for salvage of pyrimidine nucleotides, aiding the parasites biosynthesis of DNA (Al-Anouti, Quach and Ananvoranich, 2003). The *uprt* gene was initially considered as non-essential to *Toxoplasma* (Donald and Roos, 1998), with targeted disruption of the gene by non-homologous end joining allowing for selection of parasites that are resistant to FU (5-

fluorouracil) found in FUDR (Henkel et al., 2022). This method, when transfecting WT and phosphomutant GRA2 into Me49 $\Delta$ ku80 $\Delta$ GRA2 parasites, was initially seen to work better than when targeting hxppt. This is contradictory of other work, (Fox et al., 2011) argue that targeting of hxppt is a reliable strategy for generation of gene deletions in Type II parasites, of which the Me49 strain belongs to. Parasites generated here were able to show a good level of intracellular replication compared to parental strains. In addition, they were able to retain virulence levels, showing reliability of targeting this gene marker when examining Type II parasite biology. Regarding the uprt gene marker, (Bohne and Roos, 1997) show that the orientation of gene insertion when targeting uprt plays a role in bradyzoite differentiation. Transgenes in the same orientation of wildtype uprt resulted in low levels of differentiation to bradyzoites. However, a higher level of bradyzoite differentiation was seen when genes were integrated in an 'antisense' orientation. The mechanisms behind this discovery have never been explained, however it supported our choice of transgene orientation, when targeting uprt. Certainly, the transfection of phosphomutant and complemented GRA2-HA was validated with Western Blot (Fig 3A).

Both versions of phosphomutant GRA2 seemed to have little effect on the growth of tachyzoites and day 2 bradyzoites. Somewhat suggesting that phosphomutant S72 and S76 had little impact on the secondary structure of GRA2, specifically the hypothesized helix/IVN interaction. Although this could not be examined in full detail with the immunofluorescence images, transmission electron microscopy may be a more suitable method of investigating this hypothesis, as shown by (Rommereim et al., 2016). At day 7 bradyzoites we initially saw a 'shrunken' cyst phenotype in complemented GRA2 parasites. Upon also observing

the same phenotype in GRA2 phosphomutants, we deduced that this was not due as a result of phosphorylation. Instead, we determined that this phenotype was caused by the disruption of the *uprt* gene marker. This finding suggests that this selection of gene target appears to be unfavorable towards bradyzoite replication (Fig 5B).

Contributing evidence supporting such a conclusion were seen in the expected cyst structures, in the wildtype and  $\Delta$ GRA2 parasite cultures. An example of an alternative gene selection marker is Dihydrofolate reductase-thymidylate synthase (DHFR-TS) and is involved in the folic acid cycle in *Toxoplasma Gondii* (Azimi-Resketi et al., 2020). Critically, it is not known to be involved in processes regarding bradyzoite growth. Perhaps prudent then, to investigate a selection of gene markers that are less likely to inadvertently halt bradyzoite differentiation.

Experimentation with loss of the *uprt* gene marker showed that cysts were not defective in development, after 4 days bradyzoite differentiation (Bohne and Roos, 1997). Such experiments showed that in tandem with CO<sub>2</sub> deprivation, rates of bradyzoite differentiation were not reduced. This aligns with our observed data where day 2 cysts exhibited a normal phenotype. Perhaps our experimental choice of prolonged bradyzoite differentiation (7 days) resulted in the observed phenotypes in our research. This highlights an additional consideration in future work, specifically when examining bradyzoites longer than 4 days of differentiation. Bradyzoites are well known to have a lower replication rate than tachyzoites, this slower growth could rely on pyrimidine salvage pathways performed by the *uprt* gene (ILTZSCH, 1993), in the presence of CO<sub>2</sub>. Logically, prolonged disruption of such a gene and depletion of CO<sub>2</sub> could lead to nucleotide depletion, with bradyzoites in this state unable to perform replicative functions. The 'shrunk' mature cyst phenotype that we observed in our phosphomutant GRA2 experiments may be as a result of this reasoning. An

additional improvement could be to review our method of bradyzoite differentiation altogether. In our experiments, we incubated parasites at 37°C in ambient CO<sub>2</sub> to induce bradyzoite growth. As aforementioned, for prolonged incubation periods, depletion of CO<sub>2</sub> may be detrimental to bradyzoite differentiation. Alternative methods of differentiation should be implemented to circumvent the issues seen in our study. One recent study conducted by (Sanchez et al., 2023), observed bradyzoite viability and survival. Experimental methods obtained from the study show that certain parasite lines were instead exposed to heat shock. Specifically, this was done by increasing of the temperature from 37°C to 43°C for 48 hours, before returning the temperature back to 37°C - this method of heat shock was first reported by (Soete, Camus and Dubrametz, 1994). It must be concluded from our work that perhaps an alternative method of bradyzoite differentiation as exemplified above should be considered. Importantly, this may result in a more preferential environment for bradyzoites to replicate and grow for *in vitro* analysis.

Overall, our phosphomutant GRA2 data showed minor impact in cysts. However, it is impossible to rule out that regulatory mechanisms are seen later in cyst development. Future work should consider the potential alterations listed above with alternative gene marker selection and bradyzoite differentiation. Such changes could begin to examine fully the regulation of secreted proteins in chronic infection of *Toxoplasma Gondii*.

### T56 Phosphosite

Our successful mutation experiments regarding S72 and S76 allowed transfection of these phosphomutant GRA2 sequences, unfortunately SDM experiment of T56 were less fruitful. It must be noted that repeat attempts were

made to create phosphomutant T56, with optimization of SDM and transformation protocol performed. It was decided with respect to resources and time management, that our work move forward with mutant S72 and S76 GRA2. Successful creation of mutant of T56 would have allowed insight into stage specific regulation of GRA2 in *Toxoplasma Gondii*. (Young et al., 2020) show that the T56 is phosphorylated in the chronic stage, whilst S72 and S76 are phosphorylated in the acute. Successful SDM of T56 would have allowed to create phosphomutants to mimic and disrupt both stages of infection. To clarify, an example would be a bradyzoite phosphomimic – T56 residue substituted to Aspartic, with S72 and S76 substituted to Alanine. Upon successful SDM of T56, the next steps would be to extract gDNA from phosphomutant S72 and S76 parasites. Using the example above to create a bradyzoite phosphomimic, SDM primers to create Aspartic 56 could be used with the template extracted from phosphoablative S72 and S76. Hypothetically, such mutant GRA2 sequence would have all three phosphosites of significance mimicking bradyzoite stage regulation. This repeat experiment could also be repeated to recreate a mimic of tachyzoite regulation. Conducting of such experiments could better aid our understanding of how acute and chronic regulation secreted proteins.

### Creation of $\Delta$ PPM3C

Our investigation into phosphatases was devised from the hypothesis; that phosphatases play a key role in regulation of secreted proteins and potential ‘crosstalk’ between them (Mayoral et al., 2020). However, our experiments failed to create  $\Delta$ PPM3A, therefore we were unable to investigate the potential links between the two phosphatases. Coupled with the unknown impact of  $\Delta$ PPM3A on the cyst wall structure, it is recommended that this failure be rectified. Future work should be

encouraged to successfully create  $\Delta$ PPM3A, allowing the potential communication between these phosphatases to be identified.

The steps taken to create and confirm parasite cultures of  $\Delta$ PPM3C were not without problems. This involved checking whether our desired KO locus (mCherry-HXGPRT) is found in the correct place within the parasite genome. A first set of insertion check primers used to probe  $\Delta$ PPM3C populations and clones were unsuccessful, resulting in non-specific binding of the primers to various locations in the genome once extracted (data not shown). As a result, redesign of the primers was performed, they were also checked for specificity and primer dimerization via BLAST searches on [ToxoDB](#). Another improvement that was recommended was the addition of DMSO (Dimethyl Sulfoxide) to our PCR reactions. DMSO is known to reduce secondary structures, whilst increasing yield of amplified product (Cauhan, 2018). These optimization techniques were able to confirm  $\Delta$ PPM3C parasites indeed had our desired KO locus, in 1 of our isolated clones (Fig 5C) Our choice of parasite incubation (Day 2 – tachyzoite, Day 2 and 7 – bradyzoite), specifically we were hoping to build on preliminary findings by (Mayoral et al., 2020). Our hypothesis stemmed from discovery of phosphopeptides belonging to GRA2 in previous  $\Delta$ PPM3C cultures. Emphasizing that PPM3C may interact with GRA2 later than 32 hours post infection. Our data however offers no such support for the argument, GRA2 localized normally and similarly to a model proposed by (Guevara et al., 2019). This model proposes in day 2 bradyzoites, GRA2 is found to be equally located in the cyst matrix and wall, whilst more abundantly found in the cyst wall in day 7 bradyzoites. Nevertheless, even though no such relationship could be concluded with GRA2, one noticeable feature of our work is the reduced DBA staining seen at the cyst wall in day 7 bradyzoites. The clear lack of DBA staining

here leads to an attractive hypothesis – that movement and regulation of CST1 may be, in part, controlled by PPM3C. This lack of CST1 at the cyst wall is a key finding, its presence is argued to be a major component of the cysts wall, conferring durability (Tomita et al., 2013). Phosphoproteomic data from (Young et al., 2020) shows CST1 phosphosites that are phosphorylated during bradyzoite conversion (T988 and T1268). This additionally validates the need to investigate the chronic stage regulation of CST1 in closer detail. To achieve such goals, experiments could be conducted examining the above mentioned phosphosites (amongst others) creating phosphomutant CST1. This would allow examination of CST1 movement, in mature cysts. Potentially providing evidence that PPM3C is an effector that can phosphorylate CST1, causing its movement and integration into the cyst wall, post secretion. Whilst an attractive hypothesis, it is important to note, that the data in our research is a preliminary finding. Although this phenotype was consistent across all observed cysts in our work, repeat experiments should be performed with  $\Delta$ PPM3C parasites in order to truly validate this finding.

### Testing Cyst Wall Durability and Plaque Assay

Our fundamental understanding of the chronic cyst is still in development, developing methods and techniques are key and the focus of ongoing work in order to help bridge gaps in understanding. Although unconvincing in our work, plaque assays are certainly useful in *Toxoplasma* research. The key aspects of any plaque assay are to investigate invasion and replication of a strain, or isolated clone. Cyst wall proteins are now being identified as critical to the nature of the cyst. A method of assessment, to compare the effects of these genes' deletions would help fully understand the impact on parasite replication and survival. Within our work, the

purpose of acid pepsin digestion is to cause stress and release bradyzoites from the cyst structure to reinvade the monolayer of HFF's. Certain genetic deletions of key cyst wall proteins may even highlight outright killing of cysts under biochemical stress. This biochemical digestion can be argued to also mimic the natural degradation of cysts when passing through the digestive tract - although not the perfect replication of the gut (digestive tract containing proteases and enzyme digestion). Gene deletions of secreted proteins by *Toxoplasma* have already been proven to exhibit a weakened cyst structure. Data from (Tomita et al., 2013) highlights that  $\Delta$ CST1 parasites frequently showed a fragile cyst phenotype. Likely due to the reduced rigidity of the cyst wall that CST1 confers in parasites. (Guo et al., 2019) created  $\Delta$ GRA9 parasite cultures that showed a decreased ability to form plaques and argued that GRA9 is heavily involved in parasite egress in type II strains. Data from both studies supports the use of plaque assays becoming a valuable tool to examine the capabilities of *Toxoplasma Gondii*.

Unfortunately, the data that was received in our trials with acid pepsin digestion and plaque assays is not as viable. No trends could be observed, and most importantly replicated, in the data generated by the plaque assays. It was unhelpful that after no acid pepsin digestion (0 minutes) plaque numbers were not closely replicated. Although this could support the idea that spontaneity in stage conversion plays a larger role than initially thought. Nevertheless, as our aim was to assess cyst wall durability, it should be considered to remove the 0-minute incubation to avoid this confusion. The data obtained from inclusion  $\Delta$ CLP1 in the repeat experiment indicate that after 5 minutes of acid digestion, a high plaque number was observed. Whilst after 10 minutes the number of plaques had decreased hinting that cyst death may have been occurring due increasing exposure to biochemical stress. This could

indicate that CLP1 may confer a previously undescribed structural role in cysts. Unfortunately, as plaque numbers from the wildtype parasite appeared to increase between longer incubations, as opposed to the first experiment, this data is unreliable. One probable reason behind the lack of interpretable data from our experiments could lie with the high degree of interpretation in determining plaque numbers. The visualizing of negative staining was unclear and inconsistent. It is possible that dislodging of the plaques due to pipetting fixing and staining solutions occurred. Cell debris being removed as a result of staining could have also been misidentified as a plaque when counting. To make plaques clearer to observe, one improvement is provided by (Ufermann et al., 2017) in their own research comparing the efficacy of plaque assays in *Toxoplasma*. Here they argue the use of a chemically defined medium that is serum free. The chemically defined medium that was used, given the annotation DMEM, resulted in the formation of plaques that were more readily observed compared to 10% FBS plaque growth. Fetal Bovine Serum (FBS) was used in our tissue culturing experiments as well as our plaque assays. The serum is used controversially from an ethical standpoint and also expensive to manufacture (Brunner, 2010). Nevertheless, upon repeating this experiment further it should be considered to use a chemically defined medium instead of a serum containing one. A final comment regarding improving the plaque assay protocol would be to include a detailed quantitative method. qPCR with bradyzoites is something that has been conducted before, (Mayoral et al., 2019) highlights one such method. This method additionally used acid pepsin digestion as a means of biochemical digestion. Upon completion of staining and counting of plaques, the researchers conduct gDNA extraction and running of qPCR. Results from the plaque assay are then compared against a reference curve to calculate how

many genomes from parasites were allowed to form plaques in wells. One main advantage of performing qPCR here is that quantification of the total number of bradyzoites can be performed. As seen in our experiment, counting via the use of a microscope shows plaque formation is less readily identified and can be misperceived. Certainly, it should be pursued in any other further plaque assay experiments in our lab group, as a means of producing more reliable quantifiable data rather than solely counting plaque numbers. Optimization of this protocol would in time potentially could lead to the expansion of CRISPR screening. CRISPR screening when combined with plaque assays could become a powerful tool in assessing the role of essential genes in *Toxoplasma Gondii* growth and survival. This could prove to be helpful in identifying other cyst wall proteins that are vital for maintaining cyst wall rigidity. Finally, a major benefit of CRISPR screening would allow high throughput potentially allowing the simultaneous target of numerous 'essential' genes.

### Concluding Remarks

Taken together, our data recommends that alternative gene marker selection and bradyzoite differentiation are needed for research in phosphoregulation of secreted proteins in cysts. Whilst preliminary data shows potential that CST1 is impacted by the loss of PPM3C in the mature cyst wall.

### **Acknowledgements**

I would like to take the time to acknowledge all members of the lab group during the past year – Abi, Johanna and Oscar for helping me in the lab. But especially; Ksenia Bodnarenko for offering guidance when needed and specifically her expertise with immunofluorescence staining and microscopy. And importantly, Joanna Young, for supervising my project with a high degree of encouragement and willingness to support my work.

Thank You.

## Materials and Methods

### Cell Culture and Parasite Strains

Primary human foreskin fibroblasts (HFFs) (ATCC) were maintained in Dulbecco's modified Eagle's medium (DMEM) with 4.5g/liter glucose and GlutaMAX (Gibco), also added is 2% fetal bovine serum (FBS) before incubation at 37°C with 5% CO<sub>2</sub>. Me49Δku80 parasites are then maintained by growth in HFFs and dependent on parasites that were passaged every 2 to 3 days. Parasites are then sustained in respective medias dependent on strain (drug treated) For *in vitro* differentiation of bradyzoites, switch media included RPMI 1640 (Sigma-Aldrich) buffered to pH 8.2 with NaOH, 1% final FBS, 5.5g of HEPES and distilled water. Infected monolayers were then incubated at 37°C in ambient CO<sub>2</sub>, respective culture media was changed every day for optimal bradyzoite growth.

### Passaging of Parasite Lines *in vitro*

Splitting of HFF flasks infected with parasites required passaging to continue growth parasite lines but also depended on experimental requirements. This would be done every 2-3 days to avoid overgrowth and maintain healthy infection numbers.

Parasites are passaged following syringe lysis using a 21-gauge needle.

The number of drops used to seed the new flask varied but generally, 4-6 drops were used to split the parasites into the new flask of HFFs. The old flask and syringe are appropriately dispensed of with Virkon solution before the new flask is left to incubate at 37°C and 5% CO<sub>2</sub>.

### **Protein Purification**

50mL of overnight *E. coli* culture with respective plasmid was grown overnight, in Luria-Bertani (LB) broth. Before purification, the culture was spun at 3,400g for 10 minutes to obtain a bacterial pellet after removal of LB supernatant. DNA purification was then performed per manufacturer's instructions (Plasmid Midiprep Kit D4201). Final elution volumes were conducted with 200uL Nuclease Free Water.

Purification was also conducted in smaller volumes, when appropriate, involving a bacterial culture (~5mL). DNA purification was then performed per manufacturer's instructions (Monarch® Plasmid Miniprep kit, NEB T#1010). Final elution volume here was 30uL. Both methods of protein purification described above, finished in a measuring of DNA concentration (ng/μL) using NanoDrop (ThermoScientific, ND1000)

### **Gel 1% Agarose Electrophoresis**

0.5g of Agarose (Invitrogen UltraPure Agarose 16500-500) is mixed with 50mL of 1xTAE buffer (1% final gel). Dissolving of the powder was performed with the use of a microwave. 5μL of SYBR Safe Dye (ApexBio A8743) is then added before ensuring the solution completely mixed. 6-10μL of 1kb Plus DNA Ladder (NEB N0550S) is added to the first well, samples are then loaded into wells of the gel, mixed with Gel Loading Dye (purple, NEB B7025S) in a 1:6 dilution. Running of the gel is set with a manual current of 120V for 30-50 minutes. Once completed the gel is imaged with the ChemiDoc MP imaging system (BioRad 12003153)

### **Site Directed Mutagenesis (SDM) of Toxoplasma Gondii GRA2 Serine 72,76 to Alanine and Aspartic Acid**

Mutations at the S72 and S76 positions of GRA2 were introduced into pUPRT-GRA2 using guidance from the Q5<sup>®</sup> Site-Directed Mutagenesis PCR Kit (NEB E0554), to introduce Alanine and Aspartic mutations at each site. Each construct was amplified with custom designed oligonucleotide primers (listed in Table S1), these were designed to anneal in a back-to-back manner at the 5' ends containing the desired nucleotide change with the use of Phusion <sup>®</sup> Polymerase (NEB M0530S). After amplification, PCR product was digested with Dpn1 for 1 hour at 50<sup>°</sup>C before purification using (NEB) Monarch PCR and DNA Cleanup Kit (5ug) (T1030S/L). Followed by treatment with 2 $\mu$ l (NEB) T4 Ligase Buffer (B0202S) and 2 $\mu$ l (NEB) Polynucleotide Kinase (M0201S) and incubation at 37<sup>°</sup>C for 30 minutes. Final treatment of 1 $\mu$ l (NEB) T4 Ligase (M0202L) was performed at room temperature for 15-30 minutes.

### **Heat Shock Transformation**

10 $\beta$  chemically competent *E. coli* is stored at -80<sup>°</sup>C and was carefully handled to make sure thawing of bacteria occurred on ice. 10 $\mu$ L of the cloning reaction is mixed with 100 $\mu$ L of *E. coli*, before allowing to cool on ice for 25 minutes. A heat block is then set to 42<sup>°</sup>C, with cloning reactions incubated for 1 minute. 1mL of LB is added to the reactions before incubating in a heat block at 37<sup>°</sup>C and agitation setting of 300rpm, for 1 hour. LB-Agar plates supplemented with 70 $\mu$ g/mL Ampicillin are then gathered and allowed to sit at room temperature. Completion of the 1-hour incubation for the cloning reactions is then followed by a 2-minute centrifuge spin, at 6000rpm. Discarding of the supernatant is followed by resuspension of the bacterial pellet in LB. The resuspension is then spread on the plates and incubated overnight

at 37°C. Individual colonies are then prepared (Monarch® Plasmid Miniprep kit, NEB T#1010) to send for Sanger Sequencing (Azenta, Life Sciences)

### **pCas9-3' and -5' gRNA for $\Delta$ PPM3C generation**

To create  $\Delta$ PPM3C, inverse PCR using Phusion® Polymerase (NEB M0530S) was used to create 5' and 3' sgRNA targeting PPM3C and was cloned into a pSAG1-cas9 backbone (Primers listed in Table S1). PCR product was digested with Dpn1 for 1 hour at 50°C before purification using (NEB) Monarch PCR and DNA Cleanup Kit (5ug) (T1030S/L). Followed by treatment with 2µl (NEB) T4 Ligase Buffer (B0202S) and 2µl (NEB) Polynucleotide Kinase (M0201S) and incubation at 37°C for 30 minutes. Final treatment of 1µl (NEB) T4 Ligase (M0202L) was performed at room temperature for 15-30 minutes. Heat shock transformation is performed in 10 $\beta$  *E. coli* before sequence confirmation via Sanger Sequencing (Azenta, Life Sciences)

### **Parasite Transfection**

Overnight digestion of repair templates completed using (NEB) PSI-V2 restriction enzyme (R0655S) aiming for a range of 20-100µg of DNA. Following combination with 10-15 µg of respective pCas9. Phenol: chloroform cleanup is performed by Joanna Young (required only when transfecting phosphomutant/complemented GRA2). The volume of remaining DNA and plasmid is used for ethanol precipitation, this involves the adding of 1/10<sup>th</sup> volume of NaAc (3M) and 3 volumes of 96% Ethanol. Once chilled on ice for 15 minutes a spin at 14,000g for 10 minutes at 4°C is needed before the removal of supernatant. 1 volume of 70% Ethanol is added before another spin at 14,000g for 10 minutes at room temperature. The resuspension of combined DNA is completed in nuclease free H<sub>2</sub>O and P3 Primary Cell Nucleofactor Solution (Lonza, V4XP-3024). A healthy infection of  $\Delta$ GRA2

cultured parasites are then syringe lysed from a 21-gauge needle and pelleted at 17000rpm for 7 minutes and resuspended in cold 1xPBS (Sigma Dulbecco's Phosphate Buffered Saline (D8537)). 20 $\mu$ l of parasite suspension are then combined with 15 $\mu$ g DNA, a 16-well Nucleocuvette Strip is used for electroporation using 4D Nucleofactor (Lonza, AAF-1003X). Upon completion of electroporation and a 12-minute incubation at room temperature, a confluent flask of HFF's is then used to pipette the electroporated parasites into. After 24hours post transfection, FUDR (Sigma F0503-100MG) 5 $\mu$ M, was used to negatively select for transfectants.

### **Phosphatase KO generation**

An mCherry-T2A-HXGPRT fragment was amplified using primers that additionally contained 40 bp region of homology to the respective 3' and 5' UTRs of the gene of interest. Amplification was confirmed by running a small sample with 1% agarose gel electrophoresis. 10 $\mu$ g of pSAG1-cas9 respective 3' and 5' gRNAs against target and 300 $\mu$ l PCR product of mCherry-T2A-HXGPRT are then transfected into  $\sim 10^5$  Me49 $\Delta$ ku80 $\Delta$ HXGPRT tachyzoites. Drug selection media, Mycophenolic Acid (25  $\mu$ g/mL) + Xanthine (50  $\mu$ g/mL) (M/X), is then added 24 hours after to negatively select for integration of the KO locus construct. Confirming correct integration of the KO locus is conducted first with genomic extraction of successful singular cloned parasites before confirming desired insertion with insertion check primers (listed in Table S1).

### **Acid Pepsin Test**

Pepsin digestion solution (.332g Glycine, 170mM NaCl, 60mM HCL, 0.1mg/ml pepsin) is made beforehand to a temperature of 37°C. 1.5ml of filtered pepsin is added to infected flasks of the tested bradyzoite parasite lines. These were then exposed to differing time lengths of incubation (10 minutes, 5 minutes and 0

minutes). Reaction is then neutralized with 1.5ml of 1.2% Na<sub>2</sub>CO<sub>3</sub>. For plaquing, confluent monolayers in 6-well plates (Corning®, Costar ®) and wells were supplemented with 150 parasites in resuspension with respective growth medias, before incubation at 37°C with 5% CO<sub>2</sub>, for 14 days to allow for plaque growth. Important to note, that once flasks were incubating for plaquing they were not touched or moved to not disrupt growth. To help with this, they were moved to the back of the incubator.

Drug treatment test (Fig 2C) carried out with similar technique as described above, except without the use of filtered acid pepsin. Triplicate wells used per drug treatment variable. No drug treatment wells involved normal 2% FBS media with no supplemental treatment. 5uM and 10uM FUDR aliquots are made separately before 1mL dispensed in wells, identically done with 50ng/uL and 100ng/uL 6-TX. (Once 150 Me49Δku80 parasites were incubated in respective medias they were incubated for 14 days to allow for plaque growth.

### **Fixing of Plaque Assay**

For fixation of plaques, medium is aspirated before washing in 1xPBS (Sigma Dulbecco's Phosphate Buffered Saline (D8537)). Methanol solution kept at -20°C is then used to fix the wells for 5 minutes. A 1% Crystal Violet (CV) solution (12.5g of CV (TCS – HD 1295), 125mL ethanol, 500mL 1% Ammonium Oxalate (Sigma – 221716) in Water) is then used stain the wells for 10 minutes, before removal of staining with the use of distilled water. Observable plaques can then be observed and identified, with the absence of staining, under a microscope before counting and analysis.

**Genomic DNA extraction**

After observing a healthy infection of parasites in HFFs, the flask is scraped and passed through a 21-gauge needle to fully release the parasites. Pellet of parasites is then obtained after spinning at 1000g for 4-5 minutes and removal of supernatant. Manufacturer's instructions are then as followed (NEB Monarch® T#3010 kit) 50 µL Nuclease Free Water is then used to elute the sample into a clean microfuge tube before NanoDrop (ThermoScientific, ND1000) of gDNA is carried out.

**SDS – Page and Western Blott**

Expression of proteins from transfectant parasites is first resuspended in 2x Laemmli Buffer (BioRad #1610747) and analyzed with sodium sulphate polyacrylamide gel electrophoresis using a 12% polyacrylamide gel (SDS-page). Gel ran for 1 hour at 140V and used buffer 10xTGS (Tris/glycine/SDS) and Color Prestained Protein Standard Ladder (P7719S). Upon completion of gel, they were transferred to nitrocellulose membranes and then overnight incubation with 3% milk solution (Sigma-Aldrich 70166-500G). Primary antibody incubation of 1 hour 15 minutes is performed with  $\alpha$ -HA (1:1000) [Roche, 11867423001],  $\alpha$ -GRA2 (1:1000) [TG17-179 #BIO.0185], and  $\alpha$ -SFP1 (1:2000) [gift from Louis Weiss]. The membrane was then washed 3 times with PBS-0.01% Tween before the incubation of horseradish peroxidase conjugated secondary antibodies;  $\alpha$ -rat (1:5000),  $\alpha$ -mouse (1:1000) and  $\alpha$ -rabbit (1:10000) (Insight 474-1612/1806/1506). Another 3 washes of PBS-0.01% Tween happen after completion of incubation, ECL detection reagents 1 and 2 (Cytiva GERNPN2108) were then used to cover the membranes before signals are detected via ChemiDoc MP imaging system (BioRad 12003153)

### **Tachyzoite and Bradyzoite Infection of Coverslips**

Lysate from respective flasks is first obtained via syringe lysis. 10uL is taken to a hemacytometer for counting parasites. Once counted the parasites were diluted to  $1 \times 10^5$  using normal culturing media (2% FBS). 6/12 well plates with mounted coverslips are prepared, with the selective media of the infecting parasites dispensed into the wells. 100uL of the diluted parasites are then pipetted onto the coverslips before incubating at 37°C at 5% CO<sub>2</sub>. Coverslips for bradyzoite intended infections should be left to incubate for 3.5 hours before the media is changed to bradyzoite differentiation media and final incubation at 37°C and ambient CO<sub>2</sub>.

### **Fixing of Tachyzoite and Bradyzoite Coverslips**

Respective media were first removed from the wells containing parasites of interest before they were washed in 1xPBS (Sigma Dulbecco's Phosphate Buffered Saline (D8537)). 4% PFA + 0.2% Glutaraldehyde (GAH) is then used to fix the parasites with a 15-minute incubation at room temperature. Following removal of the 4% PFA + 0.2% GAH solution, more washes with PBS are completed.

### **Staining of Infected Coverslips and Immunofluorescence Microscopy**

The technique of permeabilizing parasites was dependent on whether tachyzoites or bradyzoites were being imaged. Tachyzoites required 2 minutes with 500uL of 0.1% PBS-T whilst bradyzoites require 500uL 0.2% triton, 0.1M glycine, 0.2% BSA in PBS and a 20-minute incubation on ice. Following this came 2-3 washes with PBS and then blocked for 1 hour. Infected coverslips are then probed with mouse anti-GRA2 (1:1000uL) [TG17-179 #BIO.0185], rabbit anti-GAP45 (1:10000uL) [gift from Soldati-

Favre Lab]. Secondary probing used Alexa Fluor 488-[A-28175] or 568-[A-11036] conjugated secondary antibodies (1:1000 $\mu$ L), also used was DBA, biotinylated (1:2500) [Vector Labs B-1035] and Streptavidin 660-(1:500) [Invitrogen S21377]. After coverslips were washed, they were mounted with Mounting Media (VECTASHIELD Antifade – Vector Laboratories H-1000-10) Nail varnish is used to hold the coverslips in place. Post Doc member of the lab group – Kseniia Bodnarenko then produced subsequent images with the Airyscan 2 Microscope (Zeiss LSM980) using a regular confocal mode and objective: 100x Alpha Plan Apochromat (NA.1.45 DIC)

### **Freezing of Parasite Lines**

Upon completion of successful experiments with transfectant GRA2 and PPM3C, as to keep all parasite lines for any potential further experimental use within the lab group. Respective culturing media is initially removed from the flask containing the parasite line to be frozen. Before 1.5mL of normal 2% FBS media is added, parasites here are then scraped but not syringe lysed. 1.5mL of 2x Freezing media (20% DMSO NEB – 12611P and 60% FBS, 20 % culturing media) is then added to the flask. 3mL is then split equally between 3 cryovials, cryovials are then placed in Cryo Freezing Container (Mr. Freezy – Nalgene – NL51000001). Incubated in -70°C freezer is completed overnight, before moving to appropriate box with lab group labelling the next day.

## Diagram/Figure Generation

[Benchling](#) tool was used to generate wildtype and custom designed DNA and protein sequences seen in Fig 1, [heliQuest](#) server was used to generate helical wheels and calculations of hydrophobic moment and average hydrophathy. Fig 2 and 3 uses diagrams made with [BioRender](#). Immunofluorescence image processing was conducted with Zeiss Zen 3.8 lite and ImageJ. Creation of graphs and statistical analysis performed with GraphPad Prism v8.

## References

- ADOMAKO-ANKOMAH, Y., WIER, G.M. and BOYLE, J.P. (2012). Beyond the genome: recent advances in *Toxoplasma gondii* functional genomics. *Parasite Immunology*, 34(2-3), pp.80–89. doi:<https://doi.org/10.1111/j.1365-3024.2011.01312.x>.
- Aguirre, A.A., Longcore, T., Barbieri, M., Dabritz, H., Hill, D., Klein, P.N., Lepczyk, C., Lilly, E.L., McLeod, R., Milcarsky, J., Murphy, C.E., Su, C., VanWormer, E., Yolken, R. and Sizemore, G.C. (2019). The One Health Approach to Toxoplasmosis: Epidemiology, Control, and Prevention Strategies. *EcoHealth*, 16(2), pp.378–390. doi:<https://doi.org/10.1007/s10393-019-01405-7>.
- Al-Anouti, F., Quach, T. and Ananvoranich, S. (2003). Double-stranded RNA can mediate the suppression of uracil phosphoribosyltransferase expression in *Toxoplasma gondii*. *Biochemical and Biophysical Research Communications*, [online] 302(2), pp.316–323. doi:[https://doi.org/10.1016/S0006-291X\(03\)00172-4](https://doi.org/10.1016/S0006-291X(03)00172-4).
- Almeida, F., Sardinha-Silva, A., Silva, André Moreira Pessoni, Camila Figueiredo Pinzan, Claudia, A., Cecilio, N.T., Nilmar Silvio Moretti, André R.L. Damásio, Wellington Ramos Pedersoli, José Roberto Mineo, Roberto and Maria Cristina Roque-Barreira (2015). *Toxoplasma gondii* Chitinase Induces Macrophage Activation. *PLOS One*, [online] 10(12), pp.e0144507–e0144507. doi:<https://doi.org/10.1371/journal.pone.0144507>.
- Amos, B., Aurrecochea, C., Barba, M., Barreto, A., Basenko, E., Bazant, W., Belnap, R., Blevins, A.S., Böhme, U., Brestelli, J., Brunk, B.P., Caddick, M., Callan, D., Campbell, L., Christensen, M., Christophides, G., Crouch, K., Davis, K., DeBarry, J. and Doherty, R. (2021). VEuPathDB: the eukaryotic pathogen, vector and host bioinformatics resource center. *Nucleic Acids Research*. doi:<https://doi.org/10.1093/nar/gkab929>.
- Ardito, F., Giuliani, M., Perrone, D., Troiano, G. and Muzio, L.L. (2017). The crucial role of protein phosphorylation in cell signaling and its use as targeted therapy (Review). *International Journal of Molecular Medicine*, [online] 40(2), pp.271–280. doi:<https://doi.org/10.3892/ijmm.2017.3036>.
- Attias, M., Teixeira, D.E., Benchimol, M., Vommaro, R.C., Crepaldi, P.H. and De Souza, W. (2020). The life-cycle of *Toxoplasma gondii* reviewed using animations. *Parasites & Vectors*, [online] 13(1). doi:<https://doi.org/10.1186/s13071-020-04445-z>.

Ayoade, F. and Joel Chandranesan, A.S. (2023). *HIV-1 Associated Toxoplasmosis*. [online] PubMed. Available at: <https://pubmed.ncbi.nlm.nih.gov/28722907/> [Accessed 31 May 2023].

Azimi-Resketi, M., Eskandarian, A., Ganjalikhani-Hakemi, M. and Zohrabi, T. (2020). Knocking down of the DHFR-TS gene in *Toxoplasma gondii* using siRNA and assessing the subsequences on toxoplasmosis in mice. *Acta Tropica*, 207, p.105488. doi:<https://doi.org/10.1016/j.actatropica.2020.105488>.

Bai, M.-J., Wang, J.-L., Elsheikha, H.M., Liang, Q.-L., Chen, K., Nie, L.-B. and Zhu, X.-Q. (2018). Functional Characterization of Dense Granule Proteins in *Toxoplasma Gondii* RH Strain Using CRISPR-Cas9 System. *Frontiers in Cellular and Infection Microbiology*, 8. doi:<https://doi.org/10.3389/fcimb.2018.00300>.

Bittame, A., Effantin, G., Pètre, G., Ruffiot, P., Travier, L., Schoehn, G., Weissenhorn, W., Cesbron-Delauw, M.-F., Gagnon, J. and Mercier, C. (2015). *Toxoplasma gondii*: Biochemical and biophysical characterization of recombinant soluble dense granule proteins GRA2 and GRA6. *Biochemical and Biophysical Research Communications*, [online] 459(1), pp.107–112. doi:<https://doi.org/10.1016/j.bbrc.2015.02.078>.

Bohne, W. and Roos, D.S. (1997). Stage-specific expression of a selectable marker in *Toxoplasma gondii* permits selective inhibition of either tachyzoites or bradyzoites. *Molecular and Biochemical Parasitology*, 88(1-2), pp.115–126. doi:[https://doi.org/10.1016/s0166-6851\(97\)00087-x](https://doi.org/10.1016/s0166-6851(97)00087-x).

Boothroyd, J.C., Black, M.J., Serge Bonnefoy, Hehl, A.B., Knoll, L.J., Manger, I.D., Ortega-Barria, E. and Stanislas Tomavo (1997). Genetic and biochemical analysis of development in *Toxoplasma gondii*. *The Royal Society*, 352(1359), pp.1347–1354. doi:<https://doi.org/10.1098/rstb.1997.0119>.

Bork, P., Brown, N.P., Hegyi, H. and Schultz, J. (1996). The protein phosphatase 2C (PP2C) superfamily: Detection of bacterial homologues. *Protein Science*, 5(7), pp.1421–1425. doi:<https://doi.org/10.1002/pro.5560050720>.

Bougdour, A., Braun, L., Cannella, D. and Hakimi, M.-A. (2010). Chromatin modifications: implications in the regulation of gene expression in *Toxoplasma gondii*. *Cellular Microbiology*, 12(4), pp.413–423. doi:<https://doi.org/10.1111/j.1462-5822.2010.01446.x>.

Brunner, D. (2010). Serum-free cell culture: the serum-free media interactive online database. *ALTEX*, 27(1), pp.53–62. doi:<https://doi.org/10.14573/altex.2010.1.53>.

Cauhan, T. (2018). *Role of DMSO in PCR: DMSO a PCR enhancer*. [online] Genetic Education. Available at: <https://geneticeducation.co.in/role-of-dms0-in-pcr/> [Accessed 17 Aug. 2023].

Cerutti, A., Blanchard, N. and Besteiro, S. (2020). The Bradyzoite: A Key Developmental Stage for the Persistence and Pathogenesis of Toxoplasmosis. *Pathogens*, [online] 9(3), p.234. doi:<https://doi.org/10.3390/pathogens9030234>.

Clough, B. and Frickel, E.-M. (2017). The Toxoplasma Parasitophorous Vacuole: An Evolving Host–Parasite Frontier. *Trends in Parasitology*, 33(6), pp.473–488. doi:<https://doi.org/10.1016/j.pt.2017.02.007>.

Coppens, I., Dunn, J.D., Romano, J.D., Pypaert, M., Zhang, H., Boothroyd, J.C. and Joiner, K.A. (2006). Toxoplasma gondii Sequesters Lysosomes from Mammalian Hosts in the Vacuolar Space. *Cell*, 125(2), pp.261–274. doi:<https://doi.org/10.1016/j.cell.2006.01.056>.

Dobson, S., May, T., Berriman, M., Del Vecchio, C., Fairlamb, A.H., Chakrabarti, D. and Barik, S. (1999). Characterization of protein Ser/Thr phosphatases of the malaria parasite, Plasmodium falciparum: inhibition of the parasitic calcineurin by cyclophilin-cyclosporin complex. *Molecular and Biochemical Parasitology*, [online] 99(2), pp.167–181. doi:[https://doi.org/10.1016/S0166-6851\(99\)00010-9](https://doi.org/10.1016/S0166-6851(99)00010-9).

Donald, R.G.K. and Roos, D.S. (1998). Gene knock-outs and allelic replacements in Toxoplasma gondii: HXGPRT as a selectable marker for hit-and-run mutagenesis. *Molecular and Biochemical Parasitology*, [online] 91(2), pp.295–305. doi:[https://doi.org/10.1016/S0166-6851\(97\)00210-7](https://doi.org/10.1016/S0166-6851(97)00210-7).

Dou, Z., McGovern, O.L., Di Cristina, M. and Carruthers, V.B. (2014). Toxoplasma gondii Ingests and Digests Host Cytosolic Proteins. *mBio*, 5(4). doi:<https://doi.org/10.1128/mbio.01188-14>.

Drin, G. and Antonny, B. (2009). Amphipathic helices and membrane curvature. *FEBS Letters*, 584(9), pp.1840–1847. doi:<https://doi.org/10.1016/j.febslet.2009.10.022>.

Dubey, J.P., Lindsay, D.S. and Speer, C.A. (1998). Structures of *Toxoplasma Gondii* tachyzoites, bradyzoites, and Sporozoites and Biology and Development of Tissue Cysts. *Clinical microbiology reviews*, [online] 11(2), pp.267–99. Available at: <https://www.ncbi.nlm.nih.gov/pmc/articles/PMC106833/>.

Eisenberg, D., Weiss, R.M. and Terwilliger, T.C. (1982). The helical hydrophobic moment: a measure of the amphiphilicity of a helix. *Nature*, [online] 299(5881), pp.371–374. doi:<https://doi.org/10.1038/299371a0>.

Fox, B.A., Guevara, R.B., Rommereim, L.M., Falla, A., Bellini, V., Pètre, G., Rak, C., Cantillana, V., Dubremetz, J.-F., Cesbron-Delauw, M.-F., Taylor, G.A., Mercier, C. and Bzik, D.J. (2019). *Toxoplasma gondii* Parasitophorous Vacuole Membrane-Associated Dense Granule Proteins Orchestrate Chronic Infection and GRA12 Underpins Resistance to Host Gamma Interferon. *mBio*, 10(4). doi:<https://doi.org/10.1128/mbio.00589-19>.

Frenkel, J.K. (1973). *Toxoplasma* in and around Us. *BioScience*, 23(6), pp.343–352. doi:<https://doi.org/10.2307/1296513>.

Gaji, R. Y., Sharp, A.K. and Brown, A.M. (2021). Protein kinases in *Toxoplasma gondii*. *International Journal for Parasitology*, 51(6), pp.415–429. doi:<https://doi.org/10.1016/j.ijpara.2020.11.006>.

Gautier, R., Douguet, D., Antony, B. and Drin, G. (2008). *HELIQUEST*. [online] [heliquet.ipmc.cnrs.fr](http://heliquet.ipmc.cnrs.fr). Available at: <https://heliquet.ipmc.cnrs.fr/> [Accessed 25 Jul. 2023]. a web server to screen sequences with specific  $\alpha$ -helical properties. *Bioinformatics*.

Golkar, M., Rafati, S., Abdel-Latif, M.S., Brenier-Pinchart, M.-P., Fricker-Hidalgo, H., Sima, B.K., Babaie, J., Pelloux, H., Cesbron-Delauw, M.-F. and Mercier, C. (2007). The dense granule protein GRA2, a new marker for the serodiagnosis of acute *Toxoplasma* infection: comparison of sera collected in both France and Iran from pregnant women. *Diagnostic Microbiology and Infectious Disease*, [online] 58(4), pp.419–426. doi:<https://doi.org/10.1016/j.diagmicrobio.2007.03.003>.

Guevara, R.B., Fox, B.A. and Bzik, D.J. (2020). Succinylated Wheat Germ Agglutinin Colocalizes with the *Toxoplasma gondii* Cyst Wall Glycoprotein CST1. *mSphere*, 5(2). doi:<https://doi.org/10.1128/msphere.00031-20>.

Guevara, R.B., Fox, B.A., Falla, A. and Bzik, D.J. (2019). Toxoplasma gondii Intravacuolar-Network-Associated Dense Granule Proteins Regulate Maturation of the Cyst Matrix and Cyst Wall. *mSphere*, 4(5). doi:<https://doi.org/10.1128/msphere.00487-19>.

Guo, H., Gao, Y., Jia, H., Moumouni, P.F.A., Masatani, T., Liu, M., Lee, S.-H., Galon, E.M., Li, J., Li, Y., Tumwebaze, M.A., Benedicto, B. and Xuan, X. (2019). Characterization of strain-specific phenotypes associated with knockout of dense granule protein 9 in Toxoplasma gondii. *Molecular and Biochemical Parasitology*, [online] 229, pp.53–61. doi:<https://doi.org/10.1016/j.molbiopara.2019.01.003>.

Gutte, B. and Klauser, S. (1995). 9 - *Design of Polypeptides*. [online] ScienceDirect.

Available at:

<https://www.sciencedirect.com/science/article/pii/B9780123109200500103#cesec6>

[Accessed 9 Aug. 2023].

Hargrave, K.E., Woods, S., Millington, O., Chalmers, S., Westrop, G.D. and Roberts, C.W. (2019). Multi-Omics Studies Demonstrate Toxoplasma gondii-Induced Metabolic Reprogramming of Murine Dendritic Cells. *Frontiers in Cellular and Infection Microbiology*, 9. doi:<https://doi.org/10.3389/fcimb.2019.00309>.

Henkel, S., Frohnecke, N., Maus, D., McConville, M.J., Laue, M., Blume, M. and Seeber, F. (2022). Toxoplasma gondii apicoplast-resident ferredoxin is an essential electron transfer protein for the MEP isoprenoid-biosynthetic pathway. *Journal of Biological Chemistry*, [online] 298(1), p.101468. doi:<https://doi.org/10.1016/j.jbc.2021.101468>.

Hokelek, M. (2019). Toxoplasmosis: Background, Etiology and Pathophysiology,

Epidemiology. *eMedicine*. [online] Available at:

<https://emedicine.medscape.com/article/229969-overview> [Accessed 31 May 2023].

ILTZSCH, M.H. (1993). Pyrimidine Salvage Pathways In Toxoplasma Gondii. *The Journal of Eukaryotic Microbiology*, 40(1), pp.24–28. doi:<https://doi.org/10.1111/j.1550-7408.1993.tb04877.x>.

Jacob, M.C., Favre, M. and Bensa, J.-C. (1991). Membrane cell permeabilisation with saponin and multiparametric analysis by flow cytometry. *Cytometry*, 12(6), pp.550–558.

doi:<https://doi.org/10.1002/cyto.990120612>.

Jacot, D., Fréna1, K., Marq, J.-B., Sharma, P. and Soldati-Favre, D. (2014). Assessment of phosphorylation in Toxoplasma glideosome assembly and function. *Cellular Microbiology*, 16(10), pp.1518–1532. doi:<https://doi.org/10.1111/cmi.12307>.

Jeffers, V., Tampaki, Z., Kim, K. and Sullivan, W.J. (2018). A Latent Ability to Persist: Differentiation in *Toxoplasma gondii*. *Cellular and molecular life sciences : CMLS*, [online] 75(13), pp.2355–2373. doi:<https://doi.org/10.1007/s00018-018-2808-x>.

KATO, K. (2018). How does *Toxoplasma gondii* invade host cells? *Journal of Veterinary Medical Science*, 80(11), pp.1702–1706. doi:<https://doi.org/10.1292/jvms.18-0344>.

Kotra, L.P. (2007). *Toxoplasmosis*. [online] ScienceDirect. Available at: <https://www.sciencedirect.com/science/article/pii/B9780080552323609341> [Accessed 2 Aug. 2023].

Lemgruber, L., Lupetti, P., Martins-Duarte, E.S., De Souza, W. and Vommaro, R.C. (2011). The organization of the wall filaments and characterization of the matrix structures of *Toxoplasma gondii* cyst form. *Cellular Microbiology*, 13(12), pp.1920–1932. doi:<https://doi.org/10.1111/j.1462-5822.2011.01681.x>.

Lopez, J., Bittame, A., Céline Massera, Vasseur, V., Grégory Effantin, Anne-Sylvie Valat, Célia Buillon, Allart, S., Fox, B.A., Rommereim, L.M., Bzik, D.J., Schoehn, G., Winfried Weissenhorn, Jean-François Dubremetz, Gagnon, J., Mercier, C., Marie-France Cesbron-Delauw and Blanchard, N. (2015). Intravacuolar Membranes Regulate CD8 T Cell Recognition of Membrane-Bound *Toxoplasma gondii* Protective Antigen. *Cell Reports*, 13(10), pp.2273–2286. doi:<https://doi.org/10.1016/j.celrep.2015.11.001>.

Machala, L., Kodym, P., Malý, M., Geleneky, M., Beran, O. and Jilich, D. (2015). [Toxoplasmosis in Immunocompromised patients]. *Epidemiologie, Mikrobiologie, Immunologie: Casopis Spolecnosti Pro Epidemiologii a Mikrobiologii Ceske Lekarske Spolecnosti J.E. Purkyne*, [online] 64(2), pp.59–65. Available at: <https://pubmed.ncbi.nlm.nih.gov/26099608/> [Accessed 23 Jun. 2023].

Magno, R.C., Lemgruber, L., Vommaro, R.C., De Souza, W. and Attias, M. (2005). Intravacuolar network may act as a mechanical support for *Toxoplasma gondii* inside the

parasitophorous vacuole. *Microscopy Research and Technique*, 67(1), pp.45–52.

doi:<https://doi.org/10.1002/jemt.20182>.

Manning, G. (2002). The Protein Kinase Complement of the Human Genome. *Science*, 298(5600), pp.1912–1934. doi:<https://doi.org/10.1126/science.1075762>.

Mayoral, J., Di Cristina, M., Carruthers, V.B. and Weiss, L.M. (2019). Toxoplasma gondii: Bradyzoite Differentiation In Vitro and In Vivo. *Methods in Molecular Biology*, pp.269–282. doi:[https://doi.org/10.1007/978-1-4939-9857-9\\_15](https://doi.org/10.1007/978-1-4939-9857-9_15).

Mayoral, J., Tomita, T., Tu, V., Aguilan, J.T., Sidoli, S. and Weiss, L.M. (2020). Toxoplasma gondii PPM3C, a secreted protein phosphatase, affects parasitophorous vacuole effector export. *PLOS Pathogens*, 16(12), p.e1008771.

doi:<https://doi.org/10.1371/journal.ppat.1008771>.

Mercier, C., Cesbron-Delauw, M.F. and Sibley, L.D. (1998). The amphipathic alpha helices of the toxoplasma protein GRA2 mediate post-secretory membrane association. *Journal of Cell Science*, 111(15), pp.2171–2180. doi:<https://doi.org/10.1242/jcs.111.15.2171>.

Mercier, C., Dubremetz, J.-F., Rauscher, B., Lecordier, L., Sibley, L.D. and Cesbron-Delauw, M.-F. (2002). Biogenesis of Nanotubular Network in Toxoplasma Parasitophorous Vacuole Induced by Parasite Proteins. *Molecular Biology of the Cell*, [online] 13(7), pp.2397–2409.

doi:<https://doi.org/10.1091/mbc.e02-01-0021>.

Montoya, J.G., Boothroyd, J.C. and Kovacs, J.A. (2015). 280 - *Toxoplasma gondii*. [online] ScienceDirect. Available at:

<https://www.sciencedirect.com/science/article/pii/B9781455748013002800> [Accessed 28 Jul. 2023].

Mortara, R.A., da Silva, S., Araguth, M.F., Blanco, S.A. and Yoshida, N. (1992).

Polymorphism of the 35- and 50-kilodalton surface glycoconjugates of Trypanosoma cruzi metacyclic trypomastigotes. *Infection and Immunity*, 60(11), pp.4673–4678.

doi:<https://doi.org/10.1128/iai.60.11.4673-4678.1992>.

Nam, H.-W. (2009). GRA Proteins of Toxoplasma gondii: Maintenance of Host-Parasite Interactions across the Parasitophorous Vacuolar Membrane. *The Korean Journal of Parasitology*, 47(Suppl), p.S29. doi:<https://doi.org/10.3347/kjp.2009.47.s.s29>.

Nie, L.-B., Liang, Q.-L., Du, R., Elsheikha, H.M., Han, N.-J., Li, F.-C. and Zhu, X.-Q. (2020). Global Proteomic Analysis of Lysine Malonylation in *Toxoplasma gondii*. *Frontiers in Microbiology*, 11. doi:<https://doi.org/10.3389/fmicb.2020.00776>.

Paredes-Santos, T.C., Wang, Y., Waldman, B.S., Lourido, S. and Jeroen P. J. Saeij (2019). The GRA17 Parasitophorous Vacuole Membrane Permeability Pore Contributes to Bradyzoite Viability. *Frontiers in Cellular and Infection Microbiology*, 9. doi:<https://doi.org/10.3389/fcimb.2019.00321>.

Paul, Aditya S., Saha, S., Engelberg, K., Jiang, Rays H.Y., Coleman, Bradley I., Kosber, Aziz L., Chen, C.-T., Ganter, M., Espy, N., Gilberger, Tim W., Gubbels, M.-J. and Duraisingh, Manoj T. (2015). Parasite Calcineurin Regulates Host Cell Recognition and Attachment by Apicomplexans. *Cell Host & Microbe*, 18(1), pp.49–60. doi:<https://doi.org/10.1016/j.chom.2015.06.003>.

Peixoto, L., Chen, F., Harb, O.S., Davis, P.H., Beiting, D.P., Brownback, C.S., Ouloguem, D. and Roos, D.S. (2010). Integrative Genomic Approaches Highlight a Family of Parasite-Specific Kinases that Regulate Host Responses. *Cell Host & Microbe*, 8(2), pp.208–218. doi:<https://doi.org/10.1016/j.chom.2010.07.004>.

Radke, J., Behnke, M., Mackey, A., Radke, J., Roos, D. and White, M. (2005). The transcriptome of *Toxoplasma gondii*. *BMC Biology*, 3(1), p.26. doi:<https://doi.org/10.1186/1741-7007-3-26>.

Romano, J.D., Nolan, S.J., Porter, C., Ehrenman, K., Hartman, E.J., Hsia, R.-C. and Coppens, I. (2017). The parasite *Toxoplasma* sequesters diverse Rab host vesicles within an intravacuolar network. *The Journal of Cell Biology*, [online] 216(12), pp.4235–4254. doi:<https://doi.org/10.1083/jcb.201701108>.

Rommereim, L.M., Bellini, V., Fox, B.A., Pètre, G., Rak, C., Touquet, B., Aldebert, D., Dubremetz, J.-F., Cesbron-Delauw, M.-F., Mercier, C. and Bzik, D.J. (2016). Phenotypes Associated with Knockouts of Eight Dense Granule Gene Loci (GRA2-9) in Virulent *Toxoplasma gondii*. *PloS One*, [online] 11(7), p.e0159306. doi:<https://doi.org/10.1371/journal.pone.0159306>.

- Sanchez, S.G., Bassot, E., Cerutti, A., Nguyen, M., Aïda, A., Blanchard, N. and Besteiro, S. (2023). The apicoplast is important for the viability and persistence of *Toxoplasma gondii* bradyzoites. *Proceedings of the National Academy of Sciences*, [online] 120(34), p.e2309043120. doi:<https://doi.org/10.1073/pnas.2309043120>.
- Scheffler, J.M., Schiefermeier, N. and Huber, L.A. (2014). Mild fixation and permeabilization protocol for preserving structures of endosomes, focal adhesions, and actin filaments during immunofluorescence analysis. *Methods in Enzymology*, [online] 535, pp.93–102. doi:<https://doi.org/10.1016/B978-0-12-397925-4.00006-7>.
- Shen, B., Brown, K.M., Lee, T.D. and Sibley, L.D. (2014). Efficient Gene Disruption in Diverse Strains of *Toxoplasma gondii* Using CRISPR/CAS9. *MBio*, 5(3). doi:<https://doi.org/10.1128/mbio.01114-14>.
- Sibley, L.D. and Ajioka, J.W. (2008). Population Structure of *Toxoplasma gondii*: Clonal Expansion Driven by Infrequent Recombination and Selective Sweeps. *Annual Review of Microbiology*, 62(1), pp.329–351. doi:<https://doi.org/10.1146/annurev.micro.62.081307.162925>.
- Sibley, L.D., Niesman, I.R., Parmley, S.F. and Cesbron-Delauw, M.F. (1995). Regulated secretion of multi-lamellar vesicles leads to formation of a tubulo-vesicular network in host-cell vacuoles occupied by *Toxoplasma gondii*. *Journal of Cell Science*, 108(4), pp.1669–1677. doi:<https://doi.org/10.1242/jcs.108.4.1669>.
- Sinai, A.P., Webster, P. and Joiner, K.A. (1997). Association of host cell endoplasmic reticulum and mitochondria with the *Toxoplasma gondii* parasitophorous vacuole membrane: a high affinity interaction. *Journal of Cell Science*, 110(17), pp.2117–2128. doi:<https://doi.org/10.1242/jcs.110.17.2117>.
- Singh, U., Brewer, J.L. and Boothroyd, J.C. (2002). Genetic analysis of tachyzoite to bradyzoite differentiation mutants in *Toxoplasma gondii* reveals a hierarchy of gene induction. *Molecular Microbiology*, 44(3), pp.721–733. doi:<https://doi.org/10.1046/j.1365-2958.2002.02903.x>.
- Soete, M., Camus, D. and Dubrametz, J.F. (1994). Experimental Induction of Bradyzoite-Specific Antigen Expression and Cyst Formation by the RH Strain of *Toxoplasma gondii* in

Vitro. *Experimental Parasitology*, 78(4), pp.361–370.

doi:<https://doi.org/10.1006/expr.1994.1039>.

Soete, M., Fortier, B., Camus, D. and Dubremetz, J.F. (1993). Toxoplasma gondii : Kinetics of Bradyzoite-Tachyzoite Interconversion in vitro. *Experimental Parasitology*, 76(3), pp.259–264. doi:<https://doi.org/10.1006/expr.1993.1031>.

Stelzer, S., Basso, W., Benavides Silván, J., Ortega-Mora, L.M., Maksimov, P., Gethmann, J., Conraths, F.J. and Schares, G. (2019). Toxoplasma gondii infection and toxoplasmosis in farm animals: Risk factors and economic impact. *Food and Waterborne Parasitology*, 15, p.e00037. doi:<https://doi.org/10.1016/j.fawpar.2019.e00037>.

Stray-Pedersen, B. (1993). Toxoplasmosis in Pregnancy. *Bailliere's Clinical Obstetrics and Gynaecology*, [online] 7(1), pp.107–137. doi:[https://doi.org/10.1016/s0950-3552\(05\)80149-x](https://doi.org/10.1016/s0950-3552(05)80149-x).

Sullivan, W.J. and Jeffers, V. (2012). Mechanisms of Toxoplasma gondii persistence and latency. *FEMS Microbiology Reviews*, 36(3), pp.717–733. doi:<https://doi.org/10.1111/j.1574-6976.2011.00305.x>.

Tomita, T., Bzik, D.J., Ma, Y.F., Fox, B.A., Markillie, L.M., Taylor, R.C., Kim, K. and Weiss, L.M. (2013). The Toxoplasma gondii Cyst Wall Protein CST1 Is Critical for Cyst Wall Integrity and Promotes Bradyzoite Persistence. *PLoS Pathogens*, 9(12), p.e1003823. doi:<https://doi.org/10.1371/journal.ppat.1003823>.

Tomita, T., Ma, Y. and Weiss, L. (2018). Characterization of a SRS13: a new cyst wall mucin-like domain containing protein. *Parasitology Research*, 117(8), pp.2457–2466. doi:<https://doi.org/10.1007/s00436-018-5934-3>.

Tomita, T., Tatsuki Sugi, Yakubu, R.R., Tu, V., Ma, Y. and Weiss, L.M. (2017). Making Home Sweet and Sturdy: Toxoplasma gondii ppGalNAc-Ts Glycosylate in Hierarchical Order and Confer Cyst Wall Rigidity. *MBio*, 8(1). doi:<https://doi.org/10.1128/mbio.02048-16>.

Tosetti, N., Dos Santos Pacheco, N., Soldati-Favre, D. and Jacot, D. (2019). Three F-actin assembly centers regulate organelle inheritance, cell-cell communication and motility in Toxoplasma gondii. *eLife*, 8. doi:<https://doi.org/10.7554/elife.42669>.

- Travier, L., Mondragon, R., Dubremetz, J.-F., Musset, K., Mondragon, M., Gonzalez, S., Cesbron-Delauw, M.-F. and Mercier, C. (2008). Functional domains of the Toxoplasma GRA2 protein in the formation of the membranous nanotubular network of the parasitophorous vacuole. *International Journal for Parasitology*, [online] 38(7), pp.757–773. doi:<https://doi.org/10.1016/j.ijpara.2007.10.010>.
- Treeck, M., Sanders, John L., Elias, Joshua E. and Boothroyd, John C. (2011). The Phosphoproteomes of Plasmodium falciparum and Toxoplasma gondii Reveal Unusual Adaptations Within and Beyond the Parasites' Boundaries. *Cell Host & Microbe*, 10(4), pp.410–419. doi:<https://doi.org/10.1016/j.chom.2011.09.004>.
- Tu, V., Mayoral, J., Sugi, T., Tomita, T., Han, B., Ma, Y.F. and Weiss, L.M. (2019). Enrichment and Proteomic Characterization of the Cyst Wall from *In Vitro* Toxoplasma gondii Cysts. *mBio*, 10(2). doi:<https://doi.org/10.1128/mbio.00469-19>.
- Tu, V., Yakubu, R. and Weiss, L.M. (2018). OBSERVATIONS ON BRADYZOITE BIOLOGY. *Microbes and infection*, [online] 20(9-10), pp.466–476. doi:<https://doi.org/10.1016/j.micinf.2017.12.003>.
- Ufermann, C.-M., Müller, F., Frohnecke, N., Laue, M. and Seeber, F. (2017). Toxoplasma gondii plaque assays revisited: Improvements for ultrastructural and quantitative evaluation of lytic parasite growth. *Experimental Parasitology*, 180, pp.19–26. doi:<https://doi.org/10.1016/j.exppara.2016.12.015>.
- Wang, K., Peng, E.D., Huang, A.S., Xia, D., Vermont, S.J., Lentini, G., Lebrun, M., Wastling, J.M. and Bradley, P.J. (2016). Identification of Novel O-Linked Glycosylated Toxoplasma Proteins by Vicia villosa Lectin Chromatography. *PLOS One*, 11(3), pp.e0150561–e0150561. doi:<https://doi.org/10.1371/journal.pone.0150561>.
- Weiss, L., M. (2000). The development and biology of bradyzoites of toxoplasma gondii. *Frontiers in Bioscience*, 5(1), p.d391. doi:<https://doi.org/10.2741/weiss>.
- Yang, C., Broncel, M., Dominicus, C., Sampson, E., Blakely, W.J., Treeck, M. and Arrizabalaga, G. (2019). A plasma membrane localized protein phosphatase in Toxoplasma gondii, PPM5C, regulates attachment to host cells. *Scientific Reports*, 9(1). doi:<https://doi.org/10.1038/s41598-019-42441-1>.

Yin, D., Jiang, N., Cheng, C., Sang, X., Feng, Y., Chen, R. and Chen, Q. (2022). Protein Lactylation and Metabolic Regulation of the Zoonotic Parasite *Toxoplasma gondii*. *Genomics, Proteomics & Bioinformatics*. [online]  
doi:<https://doi.org/10.1016/j.gpb.2022.09.010>.

Young, J.C., Broncel, M., Teague, H., Russell, M.R.G., McGovern, O.L., Renshaw, M., Frith, D., Snijders, A.P., Collinson, L., Carruthers, V.B., Ewald, S.E. and Treeck, M. (2020). Phosphorylation of Secreted Proteins during Acute and Chronic Stages of Infection. *MSphere*, 5(5). doi:<https://doi.org/10.1128/msphere.00792-20>.

Zhang, Y., Lai, B.S., Juhas, M. and Zhang, Y. (2019). *Toxoplasma Gondii* Secretory Proteins and Their Role in Invasion and Pathogenesis. *Microbiological Research*, 227, p.126293.  
doi:<https://doi.org/10.1016/j.micres.2019.06.003>.

## Supplemental Data

Table S1

Primer Name	Sequence	Function
GRA2 – SDM – For. Primer	TGCAGCCAGAGTGGCAGAACAACCTG	Serine 72+76 ▶ Alanine
GRA2 – SDM – Rev. Primer	CGTTGGGCAACCGGTTCTTCTGGCTC	Serine 72+76 ▶ Alanine
GRA2 – SDM – For. Primer	TGCAGACAGAGTGGCAGAACAACCTG	Serine 72+76 ▶ Aspartic
GRA2 – SDM – Rev. Primer	CGTTGGTCAACCGGTTCTTCTGGCTC	Serine 72+76 ▶ Aspartic
PPM3C 3' pCAS9 gRNA Forward	GCGGAGGACGACAGCGTCGAGTTTTAGAGCT AGAAATAGC	Cloning 3' gRNA sequence into pCas9 for PPM3CKO
PPM3C 5' pCAS9 gRNA Forward	GACCGCCTCTGGAAAGATGGGTTTTAGAGCT AGAAATAGC	Cloning 5' gRNA sequence into pCas9 for PPM3CKO
PPM3C KO insert check Forward (#1)	CGTCTTCCGCTTGCTTCACC	KO insertion check after cloning
PPM3C KO insert check Reverse (#3)	GCACAAGAATCCGAGACAGC	KO insertion check after cloning
KO Insert analysis mCh-HXGPRT Reverse (#2)	GTGTCGAAACAAGCTGACAC	Testing the mCherry and HXGPRT region to be inserted correctly.
KO Insert analysis mCh-HXGPRT Forward (#4)	GTTGCTGCTACGACTTCAAC	Testing the mCherry and HXGPRT region to be inserted correctly.

